

**Functional analysis of *Arabidopsis thaliana* major facilitator superfamily (MFS) transporters through heterologous expression in yeast**

**João Miguel Rodrigues da Silva Brazão**

Thesis to obtain the Master of Science Degree in

**Biotechnology**

**Examination Committee**

Chairperson: Professor Arsénio do Carmo Sales Mendes Fialho

Supervisor: Professor Isabel Maria de Sá Correia Leite de Almeida

Members of the Committee: Doctor Paula Duque

**November 2013**



## Acknowledgements

First, I would like to acknowledge the guidance of Professor Isabel Sá-Correia, both as my supervisor and as head of the Biological Sciences Research Group of Instituto Superior Técnico, where I had the opportunity to develop my work. I am most thankful for the support she gave me during the experimental work and the writing of this thesis. I could not fail to give a special word to Doctor Tânia Cabrito. Thank you for the advice and support through this work and all the expertise that you teach me in laboratory. I also acknowledge the collaboration of Dr. Paula Duque, from the Molecular Plant Biology Group at Instituto Gulbenkian de Ciência.

This work was financially supported by Fundação para a Ciência e a Tecnologia (FCT) (Contracts PTDC/AGR-AAM/102967/2008).

The following personal acknowledgments will be addressed in Portuguese:

Todos os membros do BSRG mostraram um forte sentido de acolhimento e simpatia, para além de uma contínua disponibilidade para ajudar sempre que precisei, deste modo quero endereçar um grande obrigado a todos.

Em primeiro lugar, quero agradecer à Professora Isabel pela oportunidade, conhecimento, orientação e paciência que me transmitiu ao longo do meu percurso, em especial na reta final. À Doutora Tânia Cabrito obrigado por todas as conversas e por todo o tempo investido a ensinar-me tudo o que eu precisei para desenvolver o meu trabalho. Um obrigado também à Cláudia Godinho por todo o apoio que me deu na execução do meu trabalho e pelo bom companheirismo que me ajudou na minha integração.

Ao Mohamed quero agradecer por todos os momentos de boa companhia e pela experiência enriquecedora que foi trabalhar com alguém de uma cultura bastante diferente da nossa. À Christina agradeço por toda a disponibilidade para discutirmos e trocar ideias.

Não poderia deixar de dizer um obrigado aos meus colegas de mestrado Ruben, Andreia e Bia que acompanharam-me nesta jornada no BSRG.

Em último, mas não menos importante, um grande obrigado à Raquel por todo o apoio nos bons e maus momentos. E em especial um grande obrigado aos meus pais, ao meu irmão e meus tios que me apoiaram e permitiram a concretização e finalização desta etapa da minha vida.

## Abstract

Membrane transport proteins can be involved in the uptake of essential nutrients or in the efflux of toxic compounds. In the present work we have used the yeast *Saccharomyces cerevisiae* as a heterologous expression system to gain insights into the role of three *Arabidopsis thaliana* putative major facilitator superfamily transporters encoded by the open reading frames *MFS10*, *MFS11* and *MFS12*, through their cloning into the plasmid pGREG576 and functional expression in yeast.

The expression of *MFS12* fused to the *GFP* gene in yeast localized the encoded transporter at the endoplasmic reticulum and plasma membranes. Its expression conferred increased susceptibility to  $\text{Cs}^+$  and  $\text{Cu}^{2+}$  and increased tolerance to  $\text{Mn}^{2+}$  and acetic acid. Yeast cells expressing the *MFS10* or *MFS11* showed fluorescent dots throughout the cytosol and increased susceptibility to  $\text{Cs}^+$  and resistance to  $\text{Mn}^{2+}$  and acetic acid. In addition, *MFS10* expression also led to increased susceptibility to  $\text{Al}^{3+}$ ,  $\text{Co}^{2+}$  and  $\text{Cu}^{2+}$ . The alternative use of the plasmid pGREG596, with a plasma membrane localization signal, was attempted to allow the localization of *MFS10*- and *MFS11*-GFP-fused proteins at plasma membrane, but protein localization was not uniformly distributed in the plasma membrane. Under these conditions, the expression of each gene led to increased susceptibility to  $\text{Cs}^{2+}$  and resistance to acetic acid. All together, results indicate that these phenotypes are of interest to be tested in the corresponding *A. thaliana* knock-out mutants or overexpression lines and to guide further studies to understand the biological function of these plant genes.

**Keywords:** *Saccharomyces cerevisiae*, *Arabidopsis thaliana*, heterologous expression, MFS transporters, resistance to acetic acid, susceptibility to  $\text{Cs}^+$ .

## Resumo

A aquisição de nutrientes ou a expulsão de compostos tóxicos da célula são processos biológicos mediados por proteínas transmembranares. O presente trabalho envolveu o estudo de três presumíveis transportadores codificados pelas grelhas de leitura aberta *MFS10*, *MFS11* e *MFS12* pertencentes à planta modelo *Arabidopsis thaliana* e incluídos na Superfamília de Facilitadores Principais. O modelo eucariota *Saccharomyces cerevisiae* foi utilizado como sistema de expressão heteróloga para a análise funcional do papel destes transportadores.

Os três genes foram clonados no vetor de clonagem pGREG576 e expressos em levedura. A expressão em levedura do gene *MFS12* fundido com o gene *GFP* mostrou que a respetiva proteína está localizada nas membranas do retículo endoplasmático e plasmática e a sua expressão conduz ao aumento da suscetibilidade ao  $\text{Cs}^+$  e  $\text{Cu}^+$  e da tolerância ao  $\text{Mn}^{2+}$  e ácido acético. Os genes *MFS10* e *MFS11* quando expressos levaram a agregados fluorescentes no citosol e a um aumento da suscetibilidade ao  $\text{Cs}^+$  e tolerância ao  $\text{Mn}^{2+}$  e ácido acético. A expressão do gene *MFS10* conduziu também a um aumento da suscetibilidade ao  $\text{Al}^{3+}$ ,  $\text{Co}^{2+}$  e  $\text{Cu}^{2+}$ . De modo a garantir uma localização na membrana plasmática dos transportadores *MFS10* e *MFS11*, foi utilizado o plasmídeo pGREG596. No entanto, as respetivas proteínas não mostraram uma localização uniforme em toda a membrana plasmática, embora a sua expressão leva-se também a um aumento da suscetibilidade ao  $\text{Cs}^+$  e da tolerância ao ácido acético. Em suma, estes resultados indicam que estes dois fenótipos são de interesse para posterior análise em mutantes de *A. thaliana* e poderão guiar estudos futuros com vista à compreensão da função destes transportadores.

**Palavras-chave:** *Saccharomyces cerevisiae*, *Arabidopsis thaliana*, expressão heteróloga, transportadores MFS, resistência a ácido acético, suscetibilidade ao  $\text{Cs}^+$ .

# Index

Acknowledgements .....	I
Abstract.....	II
Resumo .....	III
Index .....	IV
List of figures .....	VI
List of tables .....	IX
Abbreviations .....	X
<b>1. Introduction.....</b>	<b>1</b>
<b>1.1. Yeast as model eukaryote and heterologous expression host system.....</b>	<b>1</b>
1.1.1. Yeast as model eukaryote .....	1
1.1.2. Heterologous expression in yeast.....	2
<b>1.2. Transport Systems.....</b>	<b>3</b>
1.2.1. Major Facilitator Superfamily .....	4
1.2.2. <i>Saccharomyces cerevisiae</i> MFS transporters with special emphasis on those involved in multidrug resistance .....	5
1.2.3. <i>Arabidopsis thaliana</i> MFS transporters .....	9
<b>1.3. Heterologous expression of <i>A. thaliana</i> transporters in yeast to facilitate their     functional analysis: case - studies .....</b>	<b>11</b>
1.3.1. Functional analysis of transporters of the Phosphate:H <sup>+</sup> symporter family.....	11
1.3.2. Functional analysis of Zinc-Induced Facilitator Like 1 .....	16
<b>1.4. Introduction to the work described in this thesis.....</b>	<b>19</b>
<b>2. Material and Methods .....</b>	<b>21</b>
2.1. Yeast strains and growth conditions .....	21
2.2. Optimization of polymerase chain reaction conditions .....	21
<b>2.3. Cloning of <i>A. thaliana</i> <i>MFS10</i>, <i>MFS11</i> and <i>MFS12</i> genes in a yeast expression     cloning vector.....</b>	<b>22</b>
2.3.1. Drag & Drop cloning method.....	22
2.3.2. pGREG576/ pGREG596 restriction .....	24
2.3.3. Yeast transformation.....	24
2.3.4. Vector construction confirmation.....	25
2.3.5. Yeast total DNA extraction .....	25
2.3.6. <i>E. coli</i> electroporation .....	25
2.3.7. Plasmid DNA extraction .....	26
2.3.8. Plasmid DNA restriction profile .....	26
2.3.9. Plasmid DNA sequencing .....	27

2.4.	Sub-cellular GFP-fused protein localization .....	27
2.5.	Chemical stress susceptibility plate assays .....	27
3.	Results .....	29
3.1.	<i>A. thaliana</i> cDNA amplification and plasmid construction .....	29
3.1.1.	Preparation of genetic constructions in pGREG576 plasmid .....	29
3.1.2.	Preparation of genetic constructions in pGREG596 plasmid .....	30
3.2.	Sub-cellular localization assays .....	32
3.2.1.	MFS10 – GFP fusion protein sub-cellular localization.....	32
3.2.2.	MFS11 – GFP fusion protein sub-cellular localization.....	33
3.2.3.	MFS12 – GFP fusion protein sub-cellular localization.....	34
3.3.	Chemical stress susceptibility assays .....	35
4.	Discussion.....	43
5.	References .....	48

## List of figures

Figure 1.1 - A canonical major facilitator superfamily (MFS) fold. A canonical MFS fold comprises 12 TMs that are organized into two discretely folded domains, the N and C domains. Each has two inverted 3-TM repeats (Yan, 2013).....	5
Figure 1.2 – MFS-MDR transporters topology: 12-spanner (the antiporter DHA1, light blue) and 14-spanner (the antiporter DHA2, dark blue) families (Sá-Correia <i>et al.</i> , 2009). .....	6
Figure 1.3 – Qdr2p model activity. It is proposed that the export of Qdr2p physiological substrate(s) (X) may be drive by the ability of this antiporter to coupling $K^+$ . Quinidine affected the $K^+$ uptake and acidification of the cytosol by reduncing $H^+$ efflux. In this situation, the $K^+$ uptake will help the cell to counteract these deleterious effects. Qdr2p also reduces the internal concentration of quinidine by promoting, directly or indirectly, the active expulsion of the drug (Vargas <i>et al.</i> , 2007). .....	7
Figure 1.4 – The <i>S. cerevisiae</i> transporter Tpo1p. It has a plasma membrane localization and is involved in antiport of 2,4-D with $H^+$ (adapted from Teixeira <i>et al.</i> , 2013). .....	8
Figure 1.5 – Expression patterns of the nine Pht1 transporters from <i>A. thaliana</i> , based on a compilation of histological and transcriptomic data (Adapted from Nussaume <i>et al.</i> , 2011). .....	12
Figure 1.6 – <i>Pht1;9</i> expression in yeast $\Delta pho84$ mutant strain. Pht1;9 transporter exhibits Pi influx coupled with $H^+$ across plasma membrane (Teixeira <i>et al.</i> , 2013). .....	14
Figure 2.1 – Schematic representation of the basic pGREG vector system. The inducible GAL1 promoter controls the expression of tags or generated fusion proteins. Downstream of the tags a <i>HIS3</i> stuffer fragment is flanked by specific sites for recombination, <i>rec1</i> and <i>rec2</i> . The vectors contain one of the selectable yeast markers <i>URA3</i> , <i>LEU2</i> , <i>TRP1</i> and <i>HIS3</i> , the selectable <i>E. coli</i> marker <i>ampR</i> (ampicillin resistance), as well as an additional KanMX cassette flanked by <i>loxP</i> sites. Sequences of <i>rec1</i> and <i>rec2</i> used for the targeted in vivo recombination of DNA fragments into the vector, including the translated sequence encoded by the <i>rec1</i> linker between the tag and the protein of interest (Jansen <i>et al.</i> , 2005). .....	23
Figure 2.2 - Schematic representation of the pGREG576 and pGREG596 vector. The restriction sites and respective enzymes are also indicated (EUROSCARF).....	23
Figure 2.3 - Targeted recombination into pGREG vectors. First the cloning vector is cut with <i>Sall</i> , which leads to the removal of the <i>HIS3</i> stuffer fragment. Then the gene X ( <i>MFS10</i> , <i>MFS11</i> or <i>MFS12</i> ), flanked by <i>rec1</i> and <i>rec2</i> , successfully integrates the vector by homologous recombination (Jansen <i>et al.</i> , 2005).....	24
Figure 3.1 – <i>MFS10</i> sequence (1686 bp), <i>MFS11</i> sequence (1370 bp) and <i>MFS12</i> (1572 bp) sequence PCR amplification fragments.....	29
Figure 3.2 – <i>HindIII</i> restriction profile of the plasmid constructions pGREG576_ <i>MFS10</i> , pGREG576_ <i>MFS11</i> and pGREG576_ <i>MFS12</i> . .....	30

Figure 3.3 – <i>MFS10</i> sequence (1686 bp), <i>MFS11</i> sequence (1370 bp) and <i>MFS12</i> (1572 bp) sequence PCR amplification fragments.....	31
Figure 3.4 – <i>HindIII</i> restriction profile of plasmid constructions pGREG596_ <i>MFS10</i> , pGREG596_ <i>MFS11</i> and pGREG596_ <i>MFS12</i> . .....	31
Figure 3.5 – Fluorescence microscopy images of exponential-phase BY4741 cells harboring the empty vector pGREG576 (a) or pGREG596 (b).....	32
Figure 3.6 – Fluorescence microscopy images of exponential-phase BY4741 cells harboring the plasmid pGREG576_ <i>MFS10</i> (a) or pGREG596_ <i>MFS10</i> (b) after 2.5 h of galactose-induced GFP-fused protein production.....	33
Figure 3.7 – Fluorescence microscopy images of exponential-phase BY4741 cells harboring the plasmid pGREG576_ <i>MFS11</i> after 2.5 h of galactose-induced GFP-fused-protein production (a) or the plasmid pGREG596_ <i>MFS11</i> after 1.5 h of galactose-induced GFP-fused-protein protein production (b). .....	33
Figure 3.8 – Fluorescence microscopy images of exponential-phase BY4741 cells harboring plasmid pGREG576_ <i>MFS12</i> after 2.5 h of galactose-induced GFP-fused-protein production (a) and 3 h of galactose-induced GFP-fused-protein protein production (b). .....	34
Figure 3.9 - Effect of the expression of <i>MFS10</i> in yeast cells exposed to aluminum (4.5 mM). Cell suspensions used to prepare the spots were 1:5 (b) and 1:10 (c) dilutions of the cell suspension used in a. These pictures are representative of the results obtained in 3 replicates.....	35
Figure 3.10 - Effect of the expression of <i>MFS10</i> in yeast cells exposed to Co <sup>2+</sup> (1.5 mM), Cu <sup>2+</sup> (0.7 mM) and Mn <sup>2+</sup> (35 mM). Cell suspensions used to prepare the spots were 1:5 (b) and 1:10 (c) dilutions of the cell suspension used in a. These pictures are representative of the results obtained in 3 replicates.....	36
Figure 3.11 – Effect of the expression of <i>MFS11</i> and <i>MFS12</i> in yeast cells exposed to Mn <sup>2+</sup> (35 mM) and Cu <sup>2+</sup> (0.8mM). Cell suspensions used to prepare the spots were 1:5 (b) and 1:10 (c) dilutions of the cell suspension used in a. These pictures are representative of the results obtained in 3 replicates. ....	36
Figure 3.12 – Effect of the expression of <i>MFS10</i> in yeast cells exposed to Cs <sup>+</sup> (20 mM). Cell suspensions used to prepare the spots were 1:5 (b) and 1:10 (c) dilutions of the cell suspension used in a. These pictures are representative of the results obtained in 3 replicates.....	37
Figure 3.13 – Effect of the expression of <i>MFS11</i> and <i>MFS12</i> in yeast cells exposed to Cs <sup>+</sup> (25 mM). Cell suspensions used to prepare the spots were 1:5 (b) and 1:10 (c) dilutions of the cell suspension used in a. These pictures are representative of the results obtained in 3 replicates. ....	37
Figure 3.14 – Susceptibility to low potassium growth conditions of yeast cells harboring the cloning vector pGREG576 or the plasmids pGREG576_ <i>MFS10</i> , pGREG576_ <i>MFS11</i> or pGREG576_ <i>MFS12</i> . Cell suspensions used to prepare the spots were 1:5 (b) and 1:10 (c) dilutions of the cell suspension used in a. These pictures are representative of the results obtained in 3 replicates. ....	38

Figure 3.15 – Effect of the expression of <i>MFS10</i> and <i>MFS11</i> in yeast cells exposed to Cs <sup>+</sup> (25 mM). Cell suspensions used to prepare the spots were 1:5 (b) and 1:10 (c) dilutions of the cell suspension used in a. These pictures are representative of the results obtained in 3 replicates. ....	38
Figure 3.16 – Susceptibility to low potassium growth conditions of yeast cells harboring the cloning vector pGREG576 or pGREG596 and corresponding derived recombinant plasmids. Cell suspensions used to prepare the spots were 1:5 (b) and 1:10 (c) dilutions of the cell suspension used in a. ....	39
Figure 3.17 – Effect of the expression of <i>MFS10</i> , <i>MFS11</i> and <i>MFS12</i> in yeast cells exposed to acetic acid (70 mM). Cell suspensions used to prepare the spots were 1:5 (b) and 1:10 (c) dilutions of the cell suspension used in a. These pictures are representative of the results obtained in 3 replicates. ....	40
Figure 3.18 – Effect of the expression of <i>MFS10</i> in yeast cells exposed to acetic acid (70 mM). Cell suspensions used to prepare the spots were 1:5 (b) and 1:10 (c) dilutions of the cell suspension used in a. These pictures are representative of the results obtained in 3 replicates. ....	40
Figure 3.19 – Effect of the expression of <i>MFS11</i> in yeast cells exposed to acetic acid (70 mM). Cell suspensions used to prepare the spots were 1:5 (b) and 1:10 (c) dilutions of the cell suspension used in a. These pictures are representative of the results obtained in 3 replicates. ....	41
Figure 3.20 – Effect of the expression of <i>MFS10</i> in yeast cells exposed to D-mannitol (1.85 M). Cell suspensions used to prepare the spots were 1:5 (b) and 1:10 (c) dilutions of the cell suspension used in a. These pictures are representative of the results obtained in 3 replicates. ....	41
Figure 4.1 - Confocal laser scanning microscopy images of <i>A. thaliana</i> wild-type mesophyll protoplasts transiently expressing either <i>MFS10</i> -GFP (a) or <i>MFS11</i> -GFP (b). Bars = 20 μm (results supplied by our IGC collaborators). ....	43
Figure 4.2 - Confocal laser scanning microscopy images of <i>A. thaliana</i> wild-type mesophyll protoplasts transiently expressing <i>MFS12</i> -GFP. Bars = 20 mm (results supplied by our IGC collaborators). ....	44

## List of tables

Table 1.1 – <i>A. thaliana</i> ' MFS transporters described families ( <a href="http://www.membranetransport.org">www.membranetransport.org</a> ; <a href="http://plantst.genomics.purdue.edu">plantst.genomics.purdue.edu</a> ). .....	9
Table 2.1 – Range of concentrations of the tested compounds in chemical stress susceptibility assays with yeast cells harboring pGREG596_MFS10, pGREG596_MFS11, pGREG576_MFS10, pGREG576_MFS11 or pGREG576_MFS12.....	28
Table 3.1 – Fragment sizes generated by pGREG576_MFS10, pGREG576_MFS11 and pGREG576_MFS12 with HindIII (“Yeast Genome Restriction Analysis”: <a href="http://www.yeastgenome.org/cgi-bin/PATMATCH/RestrictionMapper">www.yeastgenome.org/cgi-bin/PATMATCH/RestrictionMapper</a> ).....	30
Table 3.2 – Results from chemical susceptibility spots assays. “R” or “R+” represents yeast cells that exhibited increased tolerance to certain stress due to the expression of a plant gene compared with control cells harboring the cloning vector or with yeast cells harboring a plasmid construction, respectively. “S” or “-” represents yeast cells that exhibited decreased or unaltered tolerance due to the expression of a plant gene.....	42

## Abbreviations

2,4-D	2,4 Dichlorophenoxyacetic acid
2,4-DCP	2,4-DiChloroPhenol
ABC	ATP-Binding Cassette
ACS	Anion:Cation-Symporter
ATP	Adenosine TriPhosphate
BSRg	Biological Science Research Group
DHA	Drug:H <sup>+</sup> Antiporters
DMSO	DiMethyl SulfOxide
EUROSCARF	European Saccharomyces cerevisiae ARchive for Functional analysis
GFP	Green Fluorescent Protein
IAA	Indole-3-Acetic Acid
IGC	Instituto Gulbenkian de Ciência
IST	Instituto Superior Técnico
MCP	Monocarboxylate Porter
MCPA	2-Methyl-4-ChloroPhenoxyacetic Acid
MDR	Multi Drug Resistance
MFS	Major Facilitator Superfamily
Myr	myristoylation
NNP	Nitrate/Nitrite Porter
NPA	NaphthylPhthalamic Acid
OD	Optical Density at 600nm
PCR	Polymerase Chain Reaction
PHS	Phosphate:H <sup>+</sup> Symporter
Pi	Phosphate Inorganic
SDS	Sodium Dodecyl Sulfate
SGD	Saccharomyces Genome Database
SHS	Sialate:H <sup>+</sup> Symporter
SP	Sugar Porter
TMS	TransMembrane Segments
YPD	Yeast Peptone Dextrose
ZIFL1	Zinc-Induced Facilitator Like 1

# 1. Introduction

## 1.1. Yeast as model eukaryote and heterologous expression host system

### 1.1.1. Yeast as model eukaryote

*Saccharomyces cerevisiae* was the first eukaryote to have its genome completely sequenced in 1996 (Goffeau *et al.*, 1996). Moreover, as a single cell eukaryote, it has several advantages as a research model, such as culture simplicity, rapid growth and low cost, similarly to the prokaryote model *Escherichia coli*. However it also offers several advantages compared with the prokaryote model, such as the occurrence of posttranslational modifications and an enriched endomembrane system associated to the different organelles. In other words, it has molecular, genetic and biochemical characteristics which are similar to those of higher eukaryotes (Frommer & Ninnemann, 1995; Yesilirmak & Sayers, 2009). Research in *S. cerevisiae* has strongly contributed to the development of post-genomic experimental approaches and computational tools. Currently, a large amount of biological information is accessible through public databases. For instance, *S. cerevisiae* genes and their corresponding functions have been extensively annotated and catalogued in the Saccharomyces Genome Database ([www.yeastgenome.org](http://www.yeastgenome.org); Cherry *et al.*, 2012). A large-scale biological material has also been produced, such as collections of mutants in which each yeast gene was individually deleted (EUROSCARF – <http://web.unifrankfurt.de/fb15/mikro/euroscarf>) (Kelly *et al.*, 2001). Through the use of these mutants, it is possible a fast, easy and high-throughput search for genes involved in the resistance or susceptibility to any environmental stress. For instance, the use of yeast deletion mutants has contributed to understand mechanisms of tolerance to numerous toxic compounds of biotechnological relevance (dos Santos, *et al.*, 2013).

Despite the efforts made to explore other more relevant model systems, *S. cerevisiae* continues to be the best characterized and useful eukaryotic model, which allows to easily perform molecular studies that would be more difficult to carry out in more complex and less accessible eukaryotes. Furthermore, although many physiological mechanisms do not exist in yeast, mechanisms of adaptation and resistance to chemical and environmental stresses are apparently conserved between yeast and phylogenetically distant organisms (dos Santos *et al.*, 2013; Hohmann & Mager, 2003).

The genome-wide and tolerance analyses in yeast have been successfully used to identify genes responsible for yeast response to toxic compounds of agricultural interest, which has considerable interest in plant biology. The understanding of mechanisms of tolerance to pesticides and environmental pollutants in weed and crops was enlighten by studies focusing on yeast resistance mechanisms to these compounds, such as thus involving the yeast transporters Tpo1 and Pdr5 (Teixeira & Sá-Correia, 2002; Teixeira *et al.*, 2007).

Homologs of yeast genes can also be searched for in plant models. For instance, the Tpo1p and Pdr5 homologs were searched for in the *Arabidopsis thaliana* genome sequence and it was that found that the plant homologs are also involved in herbicide resistance, as it was previous observed with the

yeast homolog transporters (Ito & Gray, 2005; Cabrito *et al.*, 2009). Moreover, *S. cerevisiae* can also play an important role as a cell host for the functional expression of foreign proteins, such as the Tpo1 homolog, the plant transporter ZIFL1 and Pht1;9 (Cabrito *et al.*, 2009; Remy *et al.*, 2012; Remy *et al.*, 2013).

### 1.1.2. Heterologous expression in yeast

Heterologous expression is the expression of a certain protein in a non native organism. The essential tools for the production of a foreign eukaryotic protein are the corresponding encoding cDNA, an appropriate vector and a biological system able to correctly transcribe and translate the cDNA into the desired functional protein. Heterologous systems should be simple and allow studies on protein functions and roles in complex mechanisms, such as metabolic reactions and membrane transport (Yesilirmak & Sayers, 2009; Desai *et al.*, 2010).

Given all the data and tools available, the yeast model is extremely attractive as a heterologous expression system. The high number of annotated genes and the possibility of using the respective yeast deletion mutant are the foundations for the most powerful feature of the yeast heterologous expression system: functional complementation. Functional complementation consists in the restoration of wild type phenotype by the expression of a foreign protein in a yeast strain lacking the putative homolog gene encoding that protein. If observed, this complementation indicates that the foreign protein has a similar function to the endogenous protein deleted in the yeast genome. Another advantage of the use of a deletion mutant strain is the elimination or decrease of the endogenous activity, thus avoiding host interference in kinetic studies (reviewed in Ton & Rao, 2004; Cabrito *et al.*, 2009). Additionally, mutations in the foreign protein may be rapidly screened for the alteration or loss of function of interest, providing clues about structure-function relationships and helping in the identification of functional domains. This strategy was employed for the functional analysis of plant ammonium transporter AtAMT1;2 through the constructs of specific mutations in its C-terminus (Newhäuser *et al.*, 2007; reviewed in Ton & Rao, 2004). Besides phenotypical analysis, the yeast model as heterologous expression host system allows an easy kinetics analysis allowing to get more insight into the functional characterization of a foreign transporter, otherwise, certain aspects of transporter activity would be hardly described (Yesilirmak & Sayers, 2009).

The first step in the heterologous expression of a plant transmembranar transporter in yeast is to choose the gene sequence. The foreign plant cDNA sequence can be prepared from a novel open reading frame (ORF) or from a close homolog to other transporter, as it was the case of Pht1 members, which were identified on the basis of their similarity with the yeast Pi transporter, Pho84 (Nussaume *et al.*, 2011). The next step is the identification of a possible yeast mutant strain for mutant complementation assays. The parental strain can also be employed as the cell host, particularly when there is no previous information about the transport activity or about a close homolog. This may happen when the chosen foreign sequence comes from a novel ORF which has no close homologs. Finally, the cDNA corresponding to the protein of interest is cloned into a yeast expression vector and transformed into a yeast strain. Growth assays, functional complementation and biochemical analysis

of the expressed protein can be easily achieved in *S. cerevisiae*. Biochemical analysis focused on the measurement of the foreign transport activity provide a straight forward way to determine enzyme kinetic parameters, influx or efflux capacity by the transport or the identification of optimal pH and temperature for enzyme activity (Ton & Rao, 2004; Yesilirmark & Sayers, 2009). Localization assays are mainly performed based on green fluorescent protein encoding gene (*GFP*), which is fused to the heterologous gene in the cloning vector construction (Guo *et al.*, 2008; Nussaume *et al.*, 2011; Remy *et al.*, 2012). Based on the above referred features, the living yeast model has been frequently used to study the transport systems of other organisms, in particular *A. thaliana*, the biological system explored in this work.

## 1.2. Transport Systems

The control of substrate movements across cytoplasmic or internal membranes is crucial for cell maintenance. The uptake of essential nutrients and ions and the efflux of end products of metabolism and deleterious substances are necessary to preserve biological activity of eukaryotic cells. To achieve this, nature has evolved a diverse system of transport proteins that mediate the translocation of ions and small hydrophilic molecules across cellular membranes (Nagata *et al.*, 2008).

The movement of ions and macromolecular molecules across cellular membranes can occur through non-mediated transport, i.e, simple diffusion or through mediated transport. The mediated transport can be divided in facilitated diffusion and active transport. The first is performed by uniporters and channels. Whereas the active transport comprise the primary and secondary transporters. The active transport systems are mainly involved in the uptake of macronutrients and efflux of several compounds (Mitchell *et al.*, 1967; Nagata *et al.*, 2008).

The so-called “primary” transporters are energy dependent (ATP) and are capable of transport  $1-10^3$  molecules/s. These transporters, such as P-type ATPases and ATP-binding cassette (ABC) have two main roles: i) solute transport in specific directions; ii) transport of ions to generate a transmembrane concentration gradient (Higgins, 1992).

The secondary transport system drives the substrate translocation by exploiting the free energy stored in the ion or solute gradients generated by primary transporters (Mitchell *et al.*, 1967; Nagata *et al.*, 2008). This system is efficient to use a few abundant molecules as common co-transporter molecules for several transport substrates. There are more than 100 types of transporters among the secondary transporter systems of all organisms. Secondary systems have evolved according to the nature of ions for which the gradients formed between the inside and outside of the cell. Most of them depend on two ions,  $\text{Na}^+$  and  $\text{H}^+$ . However the majority of solutes, including many sugars, cations, anions, metals and drugs are co-transported with  $\text{H}^+$  ions (Mitchell *et al.*, 1967; Nagata *et al.*, 2008).

The number of genes encoding transporters in *S. cerevisiae* is above 300, while in *A. thaliana* the number exceeds 1000. The number of transporters identified in each organism varies dramatically, but is approximately proportional to genome size. For instance, the majority of these genes encode

secondary transporters in both eukaryotes: in *S. cerevisiae* they comprise around 71% within all transporters, while in *A. thaliana* this value is around 64% (<http://www.membranetransport.org/>).

### 1.2.1. Major Facilitator Superfamily

The major facilitator superfamily (MFS) transporters are ubiquitous in all the three domains of life and the largest secondary transporter family. These transporters are single-polypeptide secondary carriers only capable of transporting small solutes in response to chemiosmotic ion gradient. These transporters display three distinct kinetic mechanisms: uniporters, which transport just one type of substrate and are thrilled exclusively by the substrate gradient; symporters, which translocate two or more substrates in the same direction, making use of the electrochemical gradient of one of them as the driving force; and antiporters, which transport two or more substrate types in opposite directions across the membrane (Goswitz & Brooker, 1995).

In 1993, bioinformatic efforts provided the first evidence for the secondary carrier families. Mammalian glucose facilitators, two families of drug and multidrug efflux pumps, metabolic uptake porters, organo-phosphateester:inorganic phosphate antiporters and oligosaccharide porters (including the well-studied lactose permease of *E. coli*) were all considered major facilitator superfamily transporters (Marger & Saier, 1993). Since then, the number of MFS proteins identified is continuously rising mainly due to the increasing number of genomes sequenced and analysed *in silico*. Based on phylogenetic analysis, substrate specificity and working mechanism, this superfamily is considered to contain 76 families ([www.tcdb.org](http://www.tcdb.org); Law *et al.*, 2008), with more than 10000 sequence members identified ([www.membranetransport.org](http://www.membranetransport.org)). Within these families several transported substrates had been proposed, such as monosaccharides, oligosaccharides, amino acids, peptides, vitamins, enzyme cofactors, drugs, chromophores, nucleobases, nucleosides, nucleotides, iron chelates and organic and inorganic anions and cations. However, for 17 of these families, there are no single member function where has been characterized which means that there is no evidence for the substrates transported or the possible directions of the corresponding transport (Reddy *et al.*, 2012).

The MFS proteins usually consist of around 400-600 amino acids. These proteins possess an uniform topology of two 6-transmembrane  $\alpha$ -helices repeat units connected by hydrophilic loop, but some of them have 14 transmembrane segments (Paulsen *et al.*, 1996). Both their N- and C- termini are usually located in the cytoplasm. So far, only crystal structures for bacterial MFS proteins have been reported (Abramson *et al.*, 2003; Sun *et al.*, 2012). Although these crystal structures exhibit low sequence similarity, distinct substrate specificities, and different transport coupling mechanisms, they all share a common structural fold, known as the MFS fold (figure 1.1) (Yan, 2013).

Not a single crystal structure is available for any eukaryotic MFS protein. Currently, the determination of the structure of eukaryotic MFS proteins is a major challenge, since the available structural information is mainly derived from homology modeling, which is insufficient for mechanistic elucidation and rational drug design (Yan, 2013).

MFS proteins biological activity is performed in a large spectrum of physiological processes. For instance, transporters from the sugar porter subfamily mediate the cellular uptake of glucose and other mono- and disaccharides, which make them vital for metabolism and energy homeostasis in bacteria, archaea, fungi, protozoa, plant and animals (Henderson & Maiden, 1990; Ozcan & Johnston, 1999; Buttner, 2007; Wilson-O'Brien *et al.*, 2010; Li *et al.*, 2011; Henderson & Baldwin, 2012). In humans, the well studied glucose transporters GLUT1, 2, 3 and 4 are responsible for glucose supply into organs and tissues. Changes in expression, function or localization of these human transporters are associated with various diseases, such as, De Vivo disease or Fanconi-Bickel syndrome (Brockmann, 2009; Scheffer, 2012). In bacteria and fungi, the DHA1 and DHA2 subfamilies (drug:H<sup>+</sup> antiporters 1/2) play a major role in multidrug resistance (Tirosh *et al.*, 2012; Sá-Correia & Tenreiro, 2002).

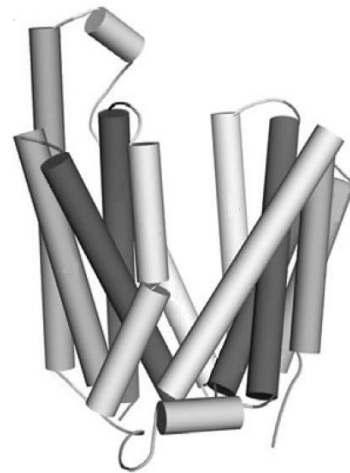


**Figure 1.1 - A canonical major facilitator superfamily (MFS) fold. A canonical MFS fold comprises 12 TMs that are organized into two discretely folded domains, the N and C domains. Each has two inverted 3-TM repeats (Yan, 2013).**

In humans, the well studied glucose transporters GLUT1, 2, 3 and 4 are responsible for glucose supply into organs and tissues. Changes in expression, function or localization of these human transporters are associated with various diseases, such as, De Vivo disease or Fanconi-Bickel syndrome (Brockmann, 2009; Scheffer, 2012). In bacteria and fungi, the DHA1 and DHA2 subfamilies (drug:H<sup>+</sup> antiporters 1/2) play a major role in multidrug resistance (Tirosh *et al.*, 2012; Sá-Correia & Tenreiro, 2002).

### **1.2.2. *Saccharomyces cerevisiae* MFS transporters with special emphasis on those involved in multidrug resistance**

The DHA1 (drug:H<sup>+</sup> antiporters 1) and DHA2 (drug:H<sup>+</sup> antiporters 2) subfamilies are involved in the multidrug resistance phenomenon. Multidrug resistance (MDR) is the simultaneous acquisition of resistance to a wide range of structurally and functionally unrelated cytotoxic chemicals (Del Sorbo, *et al.*, 2000; Jungwirth & Kuchler, 2006). The action of membrane transporters that catalyze the efflux of several distinct chemical compounds out of the cell is frequently the basis of MDR emergence (Kartner *et al.*, 1983; Del Sorbo *et al.* 2000; Hillenmeyer *et al.*, 2008; Higgins, 2007). The yeast MFS-MDR transporters, DHA1 and DHA2 function by proton antiport. The first family has the most common topology of twelve transmembrane segments, while DHA2 members have fourteen (figure 1.2) (Sá-Correia & Tenreiro, 2002).

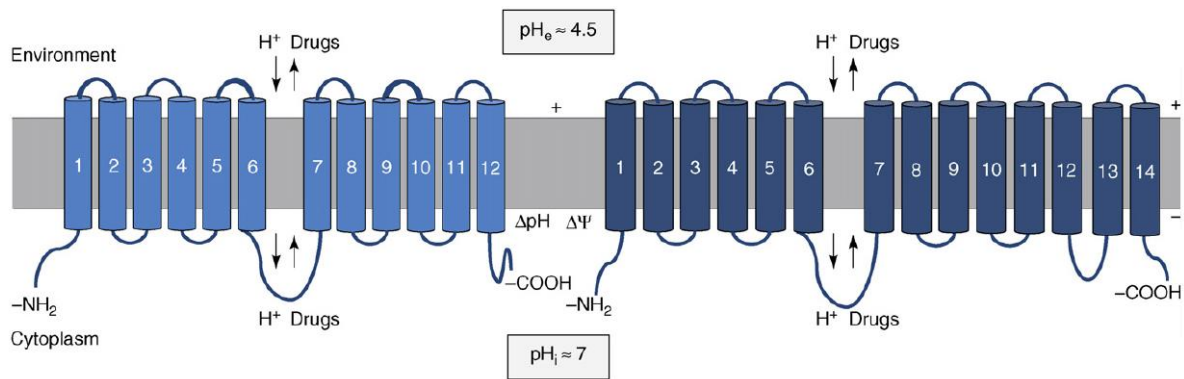


**Figure 1.2 – MFS-MDR transporters topology: 12-spanner (the antiporter DHA1, light blue) and 14-spanner (the antiporter DHA2, dark blue) families (Sá-Correia *et al.*, 2009).**

DHA1 transporters, such as, Qdr2p, Aqr1p or Tpo1p confer protection to yeast cells against compounds that usually are not present in the natural yeast environment. As it was proposed for bacterial multidrug transporters, the DHA1 findings suggested that their natural physiological role might have nothing to do with broad chemoprotection (Neyfakh, 1997; Sá-Correia *et al.*, 2009). The drugs transport might occur fortuitously or opportunistically, despite a likely existence of a natural substrate (Sá-Correia *et al.*, 2009). Several studies have contributed to support this hypothesis. For instance, the MDR Qdr2p results supported the notion that expression of *QDR2* has an important role in maintaining physiological levels of  $K^+$  in the cell. This biological function is crucial under  $K^+$  limited conditions or in the presence of quinidine. Quinidine increases the potassium requirement in yeast cells by decreasing the rate of  $K^+$  uptake and accumulation, which lead to negative effects in yeast physiology, especially in the yeast  $\Delta qdr2$  mutant (Vargas *et al.*, 2007). The Qdr2p is proposed to function as an alternative  $K^+$  transporter and might couple  $K^+$  movement with the export of its substrate, such quinidine. The Qdr2p transporter also contributes to an increase in  $H^+$  uptake following drug treatment (Vargas *et al.*, 2003). Yeast cells exposed to quinidine and suspended in slightly acidic medium exhibited a drop of the intracellular pH. This drop was due to an indirect enhancement of quinidine-inhibited  $H^+$  extrusion by the Qdr2p transporter. Despite the eventual antiport of quinidine with  $K^+/H^+$ , its transport is considered fortuitous or opportunistic (Vargas *et al.*, 2007).

Qdr2p results suggested that its normal biological activity may confer, at least in some cases, chemoprotection action through influence on proton driving force and/or internal pH, which thereby can alter the transport and partitioning of drugs (Vargas *et al.*, 2007). The altered partitioning model considers that the expression of an MDR transporter may lead to altered ion transport, indirectly affecting intracellular accumulation of the drug by perturbing plasma membrane potential and/or intracellular pH. Nevertheless, Qdr2p reduces the internal concentration of quinidine by promoting directly or indirectly, the efflux of the drug (figure 1.3) (Roepe *et al.*, 1996; Vargas *et al.*, 2007).

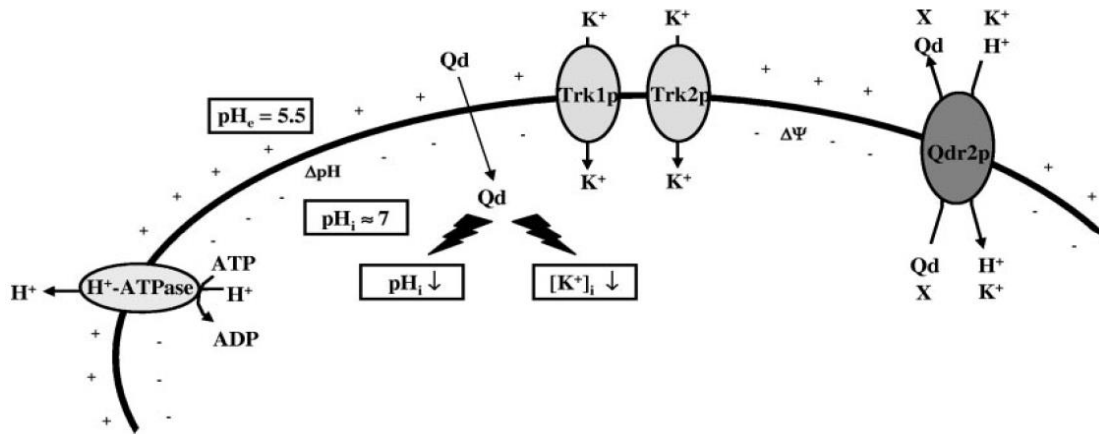


**Figure 1.3 – Qdr2p model activity.** It is proposed that the export of Qdr2p physiological substrate(s) (X) may be driven by the ability of this antiporter to couple  $K^+$  uptake and acidification of the cytosol by reducing  $H^+$  efflux. In this situation, the  $K^+$  uptake will help the cell to counteract these deleterious effects. Qdr2p also reduces the internal concentration of quinidine by promoting, directly or indirectly, the active expulsion of the drug (Vargas *et al.*, 2007).

The Aqr1p transporter is another DHA1 transporter that in addition to chemoprotection role, it shows also a natural physiological function. Aqr1p has endomembrane localization in vesicles and plasma membrane localization. This transporter is involved in the excretion of amino acids, which is important in conditions of abnormal intracellular accumulation of amino acids, such as a rapid shift to an unbalanced situation. However, its expression also confers yeast resistance to several compounds (Tenreiro *et al.*, 2002; Velasco *et al.*, 2004).

The DHA1 members Tpo1p, Tpo2p, Tpo3p and Tpo4p confer yeast resistance to toxic concentrations of polyamines (Tomitori *et al.*, 2001). Among MFS-MDR, Tpo1p is the transporter with largest number of known substrates. This transporter localizes in plasma membrane and is responsible by mediating the excretion of spermine, putrescine, spermidine, quinidine, cycloheximide, 2-methyl-4-chlorophenoxyacetic acid (MCPA), 2,4 dichlorophenoxyacetic acid (2,4-D), mycophenolic acid, nystatine, artesunate, caspofungin, indomethacin and ibuprofen (figure 1.4) (Sá-Correia, *et al.*, 2009).

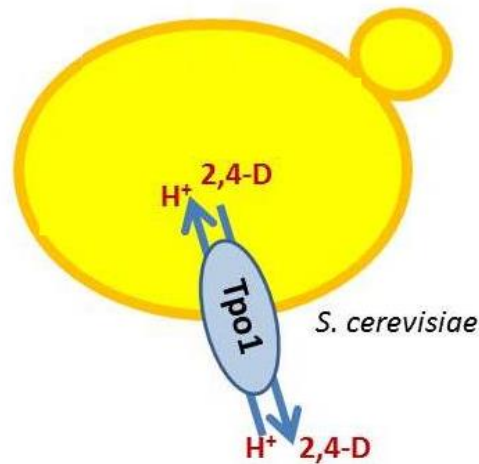


**Figure 1.4 – The *S. cerevisiae* transporter Tpo1p. It has a plasma membrane localization and is involved in antiport of 2,4-D with H<sup>+</sup> (adapted from Teixeira *et al.*, 2013).**

Although the DHA2 family comprises 10 proteins, only Sge1p, Atr1p and Azr1p transporters have been described to localize at plasma membrane and being determinants for multidrug resistance (Sá-Correia *et al.*, 2009; Tenreiro *et al.*, 2000; Kanazawa *et al.*, 1988). Other DHA2 members such as VBA1, VBA2 and VBA3 localize at vacuolar membrane and are involved in amino acid transport (Shimazu *et al.*, 2005).

Yeast MFS transporters other than those of the MFS-MDR family, include the sugar porter (SP) family, the phosphate:H<sup>+</sup> symporter (PHS) family, the sialate:H<sup>+</sup> symporter (SHS) family, the monocarboxylate porter (MCP) family and the anion:cation-symporter (ACS) family.

SP is the largest family of plasma membrane transporters in *S. cerevisiae*. One example is the group of the hexose transporters, with 18 transporters in *S. cerevisiae*. The proteins encoded by *HXT1* to *HXT4* and *HXT6* to *HXT7* are considered to be the major hexose transporters and are regulated at transcriptional level by the extracellular glucose concentration available (Reifenberger *et al.*, 1995).

So far, the phosphate:H<sup>+</sup> symporter, sialate:H<sup>+</sup> symporter, monocarboxylate porter and anion:cation-symporter families have a low number of transporters functionally characterized in yeast. For instance, Pho84p is the only phosphate transporter that belongs to the MFS family of phosphate:H<sup>+</sup> symporter. This transporter has high-affinity for phosphate and is up-regulated under phosphate limitation (Bun-Ya *et al.*, 1991).

### 1.2.3. *Arabidopsis thaliana* MFS transporters

Although the *A. thaliana* genome sequence is known since 2000, gene annotation programs are still not yet sufficient to accurately determine the function of all genes. The *A. thaliana* genome contains more than 120 genes predicted to encode MFS transporters. However, only a few transporters are described and have been essentially implicated in sugar, oligopeptide, phosphate and nitrate transport (Büttner, 2007; Mucchal *et al.*; 1996; Tsay *et al.*, 2007) (table 1.1).

**Table 1.1 – *A. thaliana*' MFS transporters described families ([www.membranetransport.org](http://www.membranetransport.org); [plantst.genomics.purdue.edu](http://plantst.genomics.purdue.edu); [www.arabidopsis.org/browse/genefamily/Monos.jsp](http://www.arabidopsis.org/browse/genefamily/Monos.jsp)).**

Transporter family	Genes	Transporter family	Genes
Monosaccharide H <sup>+</sup> symporter family	<i>STP1</i>	Phosphate:H <sup>+</sup> symporter family	<i>Pht1;1</i>
	<i>STP2</i>		<i>Pht1;2</i>
	<i>STP3</i>		<i>Pht1;3</i>
	<i>STP4</i>		<i>Pht1;4</i>
	<i>STP5</i>		<i>Pht1;5</i>
	<i>STP6</i>		<i>Pht1;6</i>
	<i>STP7</i>		<i>Pht1;7</i>
	<i>STP8</i>		<i>Pht1;8</i>
	<i>STP9</i>		<i>Pht1;9</i>
	<i>STP10</i>		<i>PHT4;1</i> <i>PHT4;2</i> <i>PHT4;3</i> <i>PHT4;4</i> <i>PHT4;5</i> <i>PHT4;6</i>
	<i>STP11</i>		
	<i>STP12</i>		
	<i>STP13</i>		
	<i>STP14</i>		
H <sup>+</sup> Symporter family for polyols and monosaccharide	<i>PLT1</i>	Nitrate/Nitrite Porter family	<i>NRT2;1</i>
	<i>PLT2</i>		<i>NRT2;2</i>
	<i>PLT3</i>		<i>NRT2;3</i>
	<i>PLT4</i>		<i>NRT2;4</i>
	<i>PLT5</i>		<i>NRT2;5</i>
	<i>PLT6</i>		<i>NRT2;6</i>
	<i>NRT2;7</i>		
Putative polyol (cyclic)-H <sup>+</sup> symporter family	<i>INT1</i>	/	
	<i>INT2</i>		
	<i>INT3</i>		
	<i>INT4</i>		
Putative monosaccharide transporter family	<i>TMT1</i>		
	<i>TMT2</i>		
	<i>TMT3</i>		
	<i>SFP1</i>		
	<i>SFP2</i>		
	<i>ERD6</i>		

The Nitrate/Nitrite Porter family NRT2 members were first discovered in the chlorate-resistant mutant of *Aspergillus nidulans* (Unkles *et al.* 1991). Following studies led to the identification of an equivalent gene family in other organisms, including *A. thaliana*. Additionally, the complete genome analysis of *A. thaliana* revealed seven NRT2 members that are differentially expressed in plant tissues (Orsel *et al.*, 2002b; Okamoto *et al.*, 2003). *AtNRT2.1* was the first *A. thaliana* NRT2 gene to be identified. *NRT2.1* was functionally characterized as being involved in high-affinity nitrate uptake (Orsel *et al.*, 2006).

Besides NRT2.1, only NRT2.2 and NRT2.4 have been functionally characterized (Cerezo *et al.*, 2001; Kiba *et al.*, 2012).

To date, the STPs represent the best characterized family of hexose transporters (within Sugar Porter family) in *A. thaliana*. All known AtSTPs are plasma membrane transporters and mediate the uptake of hexoses from the apoplastic space into the cell. AtSTP1 was the first monosaccharide transporter identified in a higher plant. It is a high-affinity monosaccharide/proton symporter capable of transporting a high range of hexoses but not fructoses. Its transcripts can be found in germinating seeds, leaves, stems, flowers, and roots. Although *AtSTP1* is expressed in various tissues, there are transporters with a more restricted localization, such as the AtSTP2, which is only present in developing pollen where it is most probably responsible for the uptake of glucose derived from callose degradation during early phases of pollen maturation (Truernit *et al.*, 1999). The expression of hexose transporters also differs in sensitivity to environmental factors, such as pathogen attack or sugar concentration. For instance, *AtSTP4* is strongly induced by wounding or bacterial and fungal elicitors (Truernit *et al.*, 1996). In summary the majority of AtSTP transporters are high-affinity monosaccharide/H<sup>+</sup> symporters localized at plasma membrane. They exhibit a large spectrum of monosaccharide substrates, except AtSTP9 which is specific for glucose (Büttner, 2007).

Within *A. thaliana* Phosphate:H<sup>+</sup> symporter family there are two families, Pht1 and Pht4. The Pht1 family is typically associated to the mediation of external phosphate, through high affinity uptake. So far the functional characterized members localize at the plasma membrane (Nussaume *et al.*, 2011). The Pht4 includes six members with Pi low-affinity capacity. Some members showed a chloroplast localization, while Pht4;6 localizes to the Golgi apparatus, where it is involved in salt tolerance (Guo *et al.*, 2008; Cubero *et al.*, 2009). Together with other phosphate transporters, Pht4 are mainly associated with internal phosphate transport.

Plant growth and development are frequently subjected to various environmental stresses. Pesticides, toxic chemicals, extreme weather conditions and infection by pathogens are critical limiting factors for plant growth. The knowledge about MFS transporters involved in abiotic stress response it is still in an early stage. Actually, only two MFS members have thus far been implicated in tolerance to abiotic stresses, the ZIF1 and ZIFL1 (Haydon & Cobbett, 2007; Cabrito *et al.*, 2009). The transporter ZIF1 was implicated in zinc tolerance (Haydon & Cobbett, 2007). The transporter ZIFL1 besides its ability to mediate efflux of auxin and auxin-related compounds, it is involved in drought stress tolerance (Cabrito *et al.*, 2009; Remy *et al.*, 2013).

Several transporters, including the MFS transporters ZIFL1 and Pht1;9 are well characterized and the heterologous expression of plant transporters in yeast has been considered crucial and extremely helpful in getting progress in the functional characterization of these plant transporters (Cabrito *et al.*, 2009; Remy *et al.*, 2012; Remy *et al.*, 2013).

### **1.3. Heterologous expression of *A. thaliana* transporters in yeast to facilitate their functional analysis: case - studies**

Plants are autotrophic organisms that fix CO<sub>2</sub> in the aerial parts and absorb mineral ions from soil through roots. Together with the photosynthetic machinery, the management of nutrients requires a regulated expression of a large set of transporters. In addition, plants are also exposed to a wide range of toxic compounds, thus requiring the activity of exporters to exclude these compounds from the cell.

A huge progress has been made in the last two decades in the study of transport processes in plants. The yeast cell as a heterologous expression host has been frequently employed to study several plant transporters. The description of these studies and approaches focused on Pht1, Pht4 and ZIFL1 functional characterized by exploiting the heterologous expression of these genes are the objective of the next part of this introduction.

#### **1.3.1. Functional analysis of transporters of the Phosphate:H<sup>+</sup> symporter family**

##### *Pht1 family*

Phosphorus is an essential nutrient for plants, playing an important role in DNA and RNA composition, membrane lipids composition and in several physiologic and metabolic processes. It is ranked as the 11<sup>th</sup> most abundant element. However its abundance in the environment is not in conformity with its uptake kinetics, mainly due to its distribution and nature. Inorganic phosphate (Pi) is the source of phosphorus for plants, preferably in the dihydrogen phosphate ion form (H<sub>2</sub>PO<sub>4</sub><sup>-</sup>), which is availability in the soil depending on microbes acquisition and cation interactions (Nussaume *et al.*, 2011). Therefore, low phosphorus availability represents a major environmental stress for plants, since it limits plant growth and consequently it has a negative impact on crops (Bieleski, 1973; Raghothama, 1999). To overcome its low availability, plants developed several strategies to regulate Pi homeostasis: phosphate re-translocation between tissues, internal recycling, symbiosis with mycorrhizal fungi, remodeling of the root system, secretion of Pi-solubilizing root exudates and induction of a high-affinity transport activity. The inorganic phosphate intracellular concentration in plant tissues is on average 5-20 mM, while in the soil is typically less than 10 μm. This concentration gradient shows the crucial role of phosphate inorganic transporters (Mimura *et al.*, 1990; Raghothama, 1999).

Several high affinity phosphate transporters were studied in the 90's, being yeast's Pho84 the first one to be identified, followed later by the discovery of their homologous in other organisms (Bun-Ya *et al.*, 1991). Although, *A. thaliana* has five types of Pi transporters, only the Pht1 and Pht4 families belong to the major facilitator superfamily. Pht1 members mediate external Pi uptake, the primary and essential step in Pi acquisition. This family is composed by nine transporters, Pht1;1-Pht1;9. They share extensive homology with each other and have been identified on the basis of their similarity with the yeast Pho84p (Nussaume *et al.*, 2011; Muchhal *et al.*, 1996). All the Pht1 proteins characterized

so far are high affinity transporters and localized at plasma membrane. However, *A. thaliana* Pht1 could have members with low-affinity activity, since barley Pht1;6 exhibited Pi uptake low-affinity (Rae *et al.*, 2003). Genome-wide analysis indicated that all members, except Pht1;6, are highly expressed in roots under Pi starvation, which suggests that these transporters are involved in the plant response to Pi starvation stress. Additionally, some Pht1 transporters are also expressed in several tissues, which suggest a likely involvement in internal Pi distribution. For instance, Pht1;5 is essential for the mobilization of Pi from P source to sink organs depending on P status of the plant (Nagarajan *et al.*, 2011) (figure 1.5).

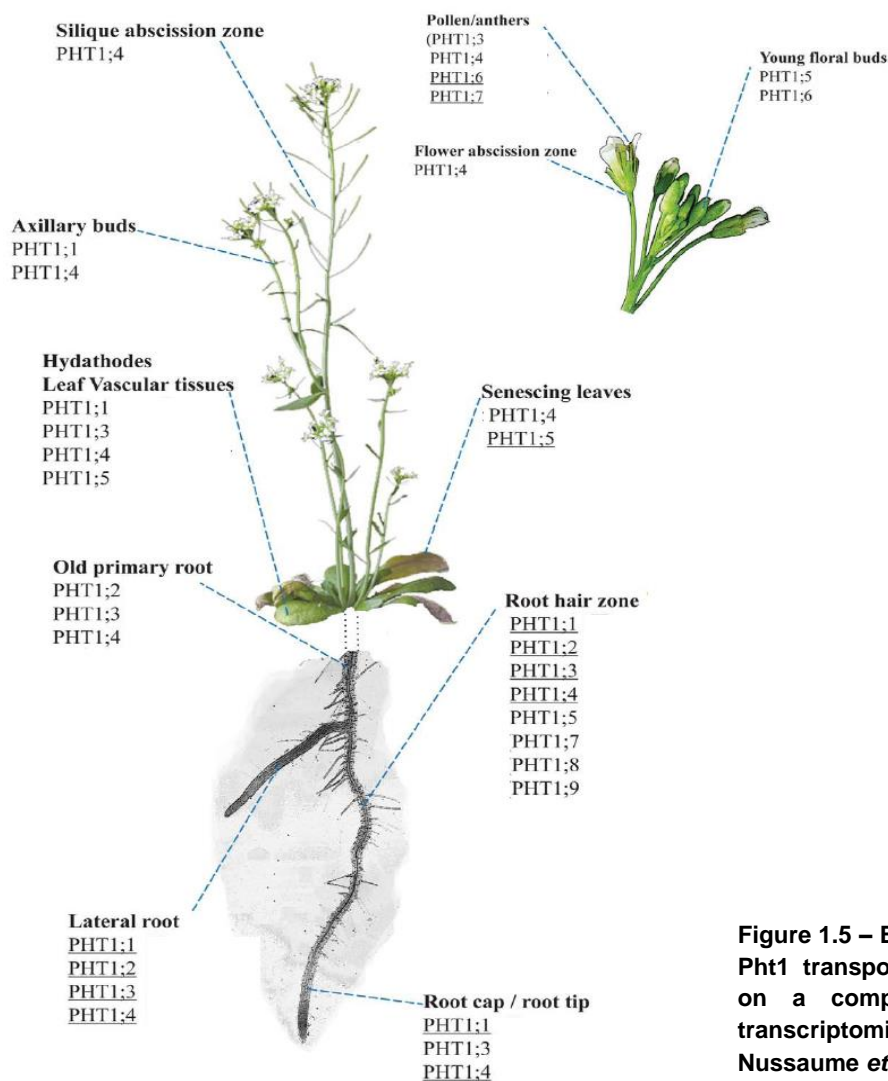


**Figure 1.5 – Expression patterns of the nine Pht1 transporters from *A. thaliana*, based on a compilation of histological and transcriptomic data (Adapted from Nussaume *et al.*, 2011).**

The first *A. thaliana* phosphate transporter identified and characterized in yeast was the Pht1;1 (Muchhal *et al.*, 1996). At this time, although the control of phosphate uptake in plants was well reported at physiological level, information on the molecular structure and genetic regulation of transport systems was poorly understood. Later the phosphate activity of Pht1;1 and also of Pht1;4 were confirmed in *A. thaliana* (Misson *et al.*, 2004; Shin *et al.*, 2004). The phosphate transporters Pht1;5, Pht1;8 and Pht1;9 were also described recently (Nagarajan *et al.*, 2011, Remy *et al.*, 2013).

In the first Pht1 study, the authors resorted to heterologous complementation of the yeast  $\Delta pho84$  mutant by plant cDNA sequence to characterize the putative Pi transporters (Muchhal *et al.*, 1996). The yeast  $\Delta pho84$  mutant became a preferable system since it lacks the phosphate high affinity transporter pho84. Two full-length *A. thaliana* cDNA sequences encoding phosphate transporters, PT1 and PT2 (actually named Pht1;1 and Pht1;2, respectively) were cloned and characterized in yeast. Expression of *Pht1;1* and *Pht1;2* in yeast  $\Delta pho84$  mutant cells complemented the deficient Pi uptake activity, showing similar performance to wild type. The phenotypical complementation together with other data of the mentioned work, such as northern, southern blots and amino acids hydrophobicity profiles of the plant cDNA sequences clearly suggested that Pht1;1 and Pht1;2 were phosphate uptake transporters (Muchhal *et al.*, 1996). Besides the first *A. thaliana* phosphate transporters expressed in yeast in 1996, more recently the Pht1;9 transporter was functionally characterized in yeast (Remy *et al.*, 2012).

Remy and collaborators described the *A. thaliana* Pht1;8 and Pht1;9 transporters. Through heterologous functional expression in yeast, sub-cellular localization studies and reverse genetics approaches in planta, it was shown that Pht1;9 mediates root Pi acquisition under Pi-deprived conditions. A double Pht1;9 /Pht1;8 silencing lines were generated to understand the role of the closest Pht1;9 homolog, Pht1;8.

Pht1;9 transporter was found to be highly expressed in roots and to localize at the plasma membrane. Its expression in roots was assessed through RT-PCR, whereas, sub-cellular localization in protoplasts and transgenic plants assays revealed that Pht1;9 localized at plasma membrane. The transporter localization in yeast cells was in agreement with plant cells localization. A plasma membrane localization of Pht1;9 in yeast cells is a prerequisite to study the plant transporter properties. Thus, the ability of Pht1;9 to complement the growth defect of the yeast  $\Delta pho84$  mutant was analysed. Expression of *Pht1;9* rescued the growth of  $\Delta pho84$  mutant cells exposed to low concentrations of Pi. Moreover,  $\Delta pho84$  cells expressing *Pht1;9* had higher Pi content, close to the same extent as in the wild type, when compared to  $\Delta pho84$  cells harboring the empty vector. A  $K_m$  of 23.6  $\mu M$ , observed in  $^{32}P$ i uptake assays, together with sub-cellular localization assays, growth complementation and Pi content analysis, clearly suggested that Pht1;9 is a high-affinity phosphate transporter localized at plasma membrane (figure 1.6) (Remy *et al.*, 2012).

To check if Pht1;9 was a Pi/ H<sup>+</sup> symporter, the authors measured the alkalization of the external medium when yeast cells expressing or not *Pht1;9* were grown in low Pi conditions. The yeast mutants carrying Pht1;9 transporter presented similar medium alkalization to wild type medium, while yeast mutant cells harboring the corresponding empty vector showed lower medium alkalization. Alkalization of the medium reflected a proton influx through the plasma membrane which was in agreement with the expected Pi/H<sup>+</sup> symporter activity (figure 1.6). Plants acquire phosphorus in its anionic form, which requires that the negative membrane potential of the plant cell must be overcome. Therefore, Pi uptake is a dynamic process that involves the activity of secondary active transporters using the proton motive force to Pi transport. The alkalization effect produced by the Pht1;9 transporter were also reported for other Pht1 transporters (Leggewie *et al.*, 1997; Mitsukawa *et al.*,

1997; Daram *et al.*,1998; Liu *et al.*,2008). Yeast cells expressing *Pht1;9* exhibited an increased susceptibility to arsenate. Besides its toxicity, arsenate is described as competing with Pi transport, which resulted in inhibitory growth effects. (Remy *et al.*, 2012)

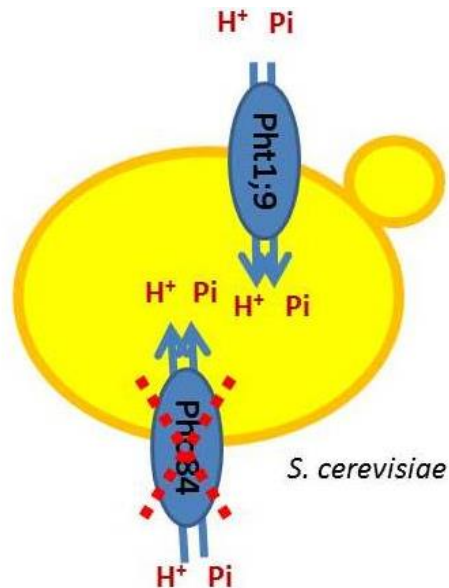


**Figure 1.6 – *Pht1;9* expression in yeast  $\Delta pho84$  mutant strain. *Pht1;9* transporter exhibits Pi influx coupled with H<sup>+</sup> across plasma membrane (Teixeira *et al.*, 2013).**

The plant root system architectural tends to suffer modifications when under Pi starvation conditions, once root branching substantially determines the ability of plant to explore soil resources. The *Pht1;9* loss-of-function *A. thaliana* lines exhibited exacerbated responses to Pi starvation, such as, a slowdown of primary root elongation and a massive lateral roots proliferation. These modifications were also correlated with an enhanced reduction of shoot biomass. Contrary to the *Pht1;9* loss of function, *Pht1;9* overexpression clearly enhances the plant resistance to Pi starvation. In Pi starvation conditions, *Pht1;9*-overexpressing plants showed a higher biomass and modifications on the root system architectural significantly attenuated, when compared to wild-type plants in the same conditions. Results obtained with the *Pht1;9* loss-of-function and *Pht1;9*-overexpressing *A. thaliana* lines exposed to toxic arsenate concentrations confirmed that *Pht1;9* mediate arsenate uptake in the native host. The set of plant results clearly indicate the phosphate uptake ability of *Pht1;9*, which confirms and highlight the contribution of the yeast model to the studies performed to clone this phosphate transporter (Remy *et al.*, 2013).

It was also proposed that *Pht1;8* has Pi uptake capacity. The double mutant *Pht1;9* /*Pht1;8* silencing lines showed a stronger Pi starvation-related phenotype compared to the plant mutant *pht1;9* loss-of-function. These results contributed to elucidate the *Pht1;8* ability transport , which also appears to play a crucial role in Pi acquisition in Pi starvation conditions (Remy *et al.*, 2012).

### *Pht4 family*

All six members of Pht4 family were functionally characterized through plants assays and heterologous expression in yeast. The presence of potential organellar targeting sequences located at the N-terminus of each Pht4 proteins led to hypothesize that some members of this family would localize to plastids (Guo *et al.*, 2008). Sub-cellular localization assays revealed that Pht4;1, Pht4;2, Pht4;4 and Pht4;5 are located in plastids membrane (Ferro *et al.*, 2003; Roth *et al.*, 2004; Guo *et al.*, 2008). The localization of Pht4;3 could not be confirmed through sub-cellular localization assays, however, based on computer-based predictions it was suggested that Pht4;3 is also targeted to plastids membrane. Pht4;6 localized at the Golgi apparatus, which was consistent that Pht4;6 N-terminal signal peptide (Emanuelsson *et al.*, 2000). *Pht4;1*, *Pht4;3*, *Pht4;4* and *Pht4;5* showed a higher expression in leaves than in roots, which suggested that the encoded proteins may function primarily in the chloroplast. However, five of the six genes were expressed at detectable levels in roots, suggesting that the encoded proteins were also targeted to heterotrophic plastids (Guo *et al.*, 2008).

To ascertain if Pht4 transporters had Pi transport functions, all the *Pht4* genes were independently expressed in the yeast PAM2 mutant strain. The PAM2 strain lacks functional copies of both high-affinity Pi transporter genes, *PHO84* and *PHO89*. The expression of the plant genes was shown to rescue the sensitive phenotype of the mutant cells under low Pi conditions. Regarding Pht4 uptake activity of other anions, as it was reported for other phosphate transporters, arsenate was showed to compete with Pi uptake. Concentration-dependent decreased in the rates of Pi transport in cells treated with a protonophore. Moreover, an optimum acidic pH required to a higher transport activity suggested that transport could be dependent on a proton-motive force.

The *Pht4* heterologous expression assay relied on Pi transport across the yeast plasma membrane. Although the transit peptide sequence determines the plastid localization, it was not necessary to delete these peptide sequences to study transport function, which suggests that these sequences are not recognized by the yeast trafficking machinery. However, the full length Pht4;1 protein was unable to complement the PAM2 mutant (Guo *et al.*, 2008). Yeast expression studies with the plastid-localized Pi transporter, Pht2;1, revealed that deletion of the transit peptide resulted in a shift in location from mitochondria membrane to plasma membrane, leading also to a large increase in transport activity (Versaw & Harrison, 2002). Thus, it was also suggested that Pht4;1 was sequestered in an internal compartment when its N-terminal sequence was not removed. Its truncated version was at least partially localized at plasma membrane, showing similar results to the other transporters (Guo *et al.*, 2008).

### 1.3.2. Functional analysis of Zinc-Induced Facilitator Like 1

The study of *ZIFL1* (*Zinc-Induced Facilitator like 1*) ability to confer yeast resistance to the synthetic auxin 2,4-D, preceded the study of *ZIFL1* role in influencing polar auxin transport and drought stress tolerance. This transporter was in a first attempt functionally characterized through heterologous expression in yeast (Cabrito *et al.*, 2009).

*ZIFL1* was chosen from a set of *TPO1* homologs based on *A. thaliana* genome screening related to 2,4-D response. The yeast homolog *TPO1* encodes a MDR-MFS plasma membrane transporter that confers increased yeast resistance to 2,4-D and it is transcriptionally activated in response to this herbicide. The *ZIFL1* functional expression was studied based on the ability to increase yeast resistance toward 2,4-D stress. The parental strain expressing the plant gene exhibited an increased growth rate and a higher final biomass under 2,4-D stress. The expression of the plant gene in the yeast  $\Delta tpo1$  strain was also able to reduce the 2,4-D-induced lag phase and to rescue the yeast growth. To assess how the transporter *ZIFL1* influences the tolerance to 2,4-D, the authors measured the intracellular accumulation of this herbicide, through [<sup>14</sup>C]-2,4-D accumulation analysis. The expression of the plant transporter led to an increased of the yeast basal ability to reduce the intracellular concentration of 2,4-D. The intracellular accumulation of 2,4-D in  $\Delta tpo1$  strain expressing the plant gene was similar to the parental strain harboring an empty vector, which showed that *ZIFL1* was able to complement the absence of Tpo1p. Given these results the authors proposed that the *ZIFL1* transporter is directly or indirectly involved in the extrusion of the 2,4-D counter-ion from yeast cells. The *TPO1* gene is a determinant of multidrug resistance in yeast, conferring yeast tolerance to diverse compounds of agro-economical importance. Given this, it was analyzed the ability of *ZIFL1* to confer resistance to pesticides and chemical compounds already related to *TPO1*. The expression of the plant gene was able to confer increased resistance to IAA, Al<sup>3+</sup> and Ti<sup>3+</sup>. This first study with *ZIFL1* suggested that this plant transporter may play a role in toxic tolerance by mediating the efflux of herbicides and toxic ions (Cabrito *et al.*, 2009).

Several components of polar auxin transporter system have been discovered through physiological studies with the exogenous source of auxin, 2,4-D (Bennett *et al.*, 1996). Remy and collaborators investigated the *in vivo* roles of *ZIFL1* transporter in auxin processes. The plant hormone auxin has a critical role in the spatial and temporal coordination of plant development, being involved in processes, such as embryo, root and vascular patterning, postembryonic organogenesis and tropisms, by directing cell division and expansion (reviewed in Woodward & Bartel, 2005). The *in vivo* analysis of *ZIFL1* transporter in *A. thaliana* and new experiments with *S. cerevisiae* through heterologous expression revealed a dual function of *ZIFL1*, polar auxin transport and drought stress tolerance (Remy *et al.*, 2013).

The dual function is determined by alternative splicing of the plant gene, allowing a varied localization and function. *ZIFL1* generates three distinct transcripts: *ZIFL1.1*, *ZIFL1.2* and *ZIFL1.3*. The first one corresponds to the full-size transporter with 12 membrane-spanning segments. *ZIFL1.2* is a truncated protein that lacks two N-terminal membrane-spanning segments. The third transcript, *ZIFL1.3* results

from a selection of an alternative splice in the fourteenth intron, which leads to the formation of a truncated protein that lacks two C-terminal membrane-spanning segments (Remy *et al.*, 2013).

Expression pattern analysis revealed that the ZIFL1 promoter is particularly active in root tissues and stomatal guard cells. Additionally, the *ZIFL1* transcripts have significant expression in leaves, while roots exclusively express *ZIFL1.1* and *ZIFL1.2* transcripts. At the sub-cellular level ZIFL1.1 transporter was localized at the tonoplast, while the truncated ZIFL1.3 transporter was localized at the plasma membrane (Remy *et al.*, 2013).

The study of the biological role of ZIFL1 transporter was initiated by phenotypical analysis through *zifl1* loss-of-function mutants. The mutant plants were hypersensitive to drought stress, since the stomatal pore was significantly larger in the *zifl1* mutants, which indicates that this transporter is required for efficient stomatal closure (Remy *et al.*, 2013). Guard cells are essential to optimize CO<sub>2</sub> uptake and concomitant water loss by accurately controlling stomata apertures in response to physiological and environmental stimuli (reviewed in Araújo *et al.*, 2011).

Due to the high expression of *ZIFL1* in roots and to the previous yeast heterologous expression (Cabrito *et al.*, 2009), it was assessed the response of roots to 2,4-D and IAA. The sensitivity revealed by the plant mutants to these compounds confirmed that the ZIFL1 transporter confers increased resistance to 2,4-D and IAA. Moreover, the plant mutants also showed a range of auxin-related defects. ZIFL1.1 complementation abolished root *zifl1* mutant defects but had no effect on their water loss rates, while ZIFL1.3 fully complemented the drought-related phenotype but not the auxin-related defects. When the influence of these transporters on cellular auxin levels was investigated, the accumulation of [<sup>14</sup>C]2,4-D and [<sup>14</sup>C]IAA was found to increased in *zifl1* mutant root tips. ZIFL1.1-overexpressing and ZIFL1.3-overexpressing lines showed decreased auxin compounds; however the last plant line showed a weaker ability to decrease the accumulation. These results were reinforced by re-examination of the auxin transport in yeast cells. Yeast *Δtpo1* mutant cells expressing *ZIFL1.1* or *ZIFL1.3* exhibited higher final biomass and a shorter lag phase in the presence of 2,4-D or IAA, when compared to *Δtpo1* mutant yeast cells harboring an empty vector. This increased resistance was correlated with a significant reduction in [<sup>14</sup>C] 2,4-D and [<sup>14</sup>C] IAA accumulation (Remy *et al.*, 2013).

The balance between cellular influx and efflux of auxin regulates the accumulation of auxin. Thus, when the IAA efflux was measured, *zifl1* mutant root tips accumulated more IAA as a result of decreased efflux, while ZIFL1.1-overexpressing lines showed the lowest accumulation of auxin, due to higher IAA efflux rates. These results clearly showed that ZIFL1.1 influences cellular IAA efflux (Remy *et al.*, 2013).

Authors verified that the modulation of auxin transport by ZIFL1.1 may not be direct. It was hypothesized that ZIFL1.1 might affect polar auxin transport by influencing the activity of the major auxin efflux carrier PIN2, reflecting an indirect auxin modulation. This may happen by modulation of PIN2 steady-state levels at the plasma membrane through interference with its vacuolar targeting or degradation. Alternatively, PIN2 activity could be also influenced by changes in plasma membrane electrochemical potential. Indeed, yeast extracellular and plant vacuolar acidification assays pointed

that polar auxin transport may be facilitated by ZIFL1.1 transporter due to an enhanced protons release from the vacuole. This would be reflected in an increase of  $H^+$  available for plasma membrane ATPases and in a proton-driving force increase for cellular auxin transport (Remy *et al.*, 2013).

The heterologous expression results showed that ZIFL1.1 is able to mediate IAA efflux in yeast (Cabrito *et al.*, 2009; Remy *et al.*, 2013). This feature is in agreement with several studies, where auxin transport activity was demonstrated in heterologous systems (Geisler *et al.*, 2005; Yang *et al.*, 2006; Blakeslee *et al.*, 2007; Yang & Murphy, 2009). Thus, the activation of other endogenous yeast transporters that can catalyze auxin efflux can be a plausible explanation for the indirect influence of ZIFL1 in auxin transport. Regarding this, the authors tested the polar auxin efflux inhibitor naphthylphthalamic acid (NPA). In plants it was shown that this inhibitor affects auxin processes. However, in yeast cells expressing *ZIFL1.1*, the IAA transport was unaffected by NPA. On the contrary, IAA export activity mediated by *PIN2* expression in yeast was clearly NPA sensitive (Petrásek *et al.*, 2006; Blakeslee *et al.*, 2007). These findings supported the idea that ZIFL1.1 transporter mediate auxin transport through activation of endogenous yeast transporters and thereby reinforce the idea that ZIFL1.1 mediate auxin-related processes in a non direct manner (Remy *et al.*, 2013).

The yeast experiments showed that the effect of *ZIFL1* expression is not restricted to auxin compounds. The response of  $\Delta tpo1$  mutant yeast cells expressing either *ZIFL1.1* or *ZIFL1.3* to various additional compounds was also tested. Besides the ability of ZIFL1.3 to confer increased yeast resistance to  $Al^{3+}$  and  $Tl^{3+}$  already reported (Cabrito *et al.*, 2009), *ZIFL1.1* and *ZIFL1.3* expression were shown to confer increased resistance to the weak acids, L-malic acid and acetic acid. It was also found that both isoforms are able to confer increased yeast susceptibility when exposed to  $Cs^+$ . This cation metal has chemical properties similar to potassium and it has been reported that  $Cs^+$  competes with potassium uptake, which is reflected in potassium starvation (Hampton *et al.*, 2004; Qi *et al.*, 2008). Therefore, complementation experiments with the yeast mutant  $\Delta qdr2$  strain were performed. Both isoforms were able to alleviate the pronounced growth defect induced by loss of *Qdr2* under  $K^+$  deprivation. It was also revealed that both isoforms have  $H^+$ -coupled  $K^+$  transport activity (Remy *et al.*, 2013). The ability to mediate potassium transport by ZIFL1.1 was suggested to rely on its ability to generate ionic and electric gradients that would favor auxin efflux through specific transporters (Vicente-Agullo *et al.*, 2004, Remy *et al.*, 2013). Concerning ZIFL1.3, its ability to mediate  $K^+$  transport is consistent with its function in stomatal movements regulation (Remy *et al.*, 2013).

This interesting study suggested that ZIFL1, through different isoforms, is able to regulate the stomatal movements and the polar auxin transport by modulating potassium and proton fluxes in *A. thaliana* cells (Remy *et al.*, 2013). Once more, Remy and collaborators took a great advantage of the yeast model, and used it to get more insight into the biological role of ZIFL1 transporter.

#### 1.4. Introduction to the work described in this thesis

The work described in this thesis is part of a joint research line involving the Biological Science Research Group (BSRG) of Instituto Superior Técnico and the Plant Molecular Biology of Instituto Gulbenkian de Ciência.

Over the years, the BSRG has given an important contribute to the research field of the yeast global response to environmental insults. The exploitation of omics (transcriptomic or proteomic) approaches together with the study of transmembranar transporters and transmembrane transport in the yeast model have been intensively used in the characterization of stress response and tolerance mechanisms. The functional analysis of yeast multidrug resistance transporters of the major facilitator superfamily has been one of the focus of a number of research programmes. The universal easy-to-manipulate yeast model has allowed the screening of a wide range of susceptibility or tolerance phenotypes and the study of the kinetics of the transport of the translocated substrates. Besides, the apparently conserved mechanisms of tolerance to chemical and environmental stresses between yeast and phylogenetically distant organisms have also promoted yeast as a model to study transport mechanisms of agricultural interest. This has been achieved through genome-wide approaches and the analysis of the mechanisms underlying yeast tolerance to these stresses as well as a heterologous expression system host. Therefore, the large experience acquired and all the advantages exhibited by the eukaryote model *S. cerevisiae* together with the plant molecular biology expertise from the Plant Molecular Biology group lead by Dr Paula Duque, led to a number of recent contributions to uncover the role of MFS transporters in plant tolerance to abiotic stress, in particular the *A. thaliana* transporters ZIFL1, Pht1;9 and its close homolog Pht1;8.

The *TPO1 A. thaliana* homolog, ZIFL1, was expressed and functionally characterized in yeast cells, where it led to increased yeast resistance to auxin and auxin-related herbicides and metal ions (Cabrito *et al.*, 2009). Recent results from the *in vivo* study of the role of ZIFL1 showed that it has the ability to mediate the efflux of the plant hormone auxin and is involved in drought stress tolerance (Remy *et al.*, 2013). The transporters Pth1;8 and Pht1;9 were identified on the basis of their similarity with Pho84, a high affinity *S. cerevisiae* phosphate transporter. Functional and biochemical analysis of Pht1;9 expressed both in yeast and in plant allowed the confirmation of the capacity of this transporter to mediate high affinity phosphate uptake (Remy *et al.*, 2012).

This thesis project intends to get insights into the biological role of the *A. thaliana* open reading frames *MFS10*, *MFS11* and *MFS12* encoding putative membrane transporters. *MFS10* protein is a close homolog of a zinc-induced facilitator 2 transporter, which was recently related to plant tolerance to high zinc concentrations (Remy *et al.*, unpublished). Additionally, publicly available microarray data indicates that *MFS10* transcript is up-regulated by high concentrations of selenium and cadmium (Zimmermann *et al.*, 2004). *MFS11*, besides having a nucleotide sequence closely related to ZIF1 and ZIFL1 transporters, its transcripts level is increased in response to osmotic, drought and salt stress (Zimmermann *et al.*, 2004). *MFS12* predicted to encode an oligopeptide transporter is highly up-regulated under iron deprivation as suggested by microarray data (Zimmermann *et al.*, 2004). The

above referred data indicated that these three putative transporters are potential candidates to be involved in plant tolerance to abiotic stress. Indeed drought, high salinity, iron availability and presence of pollutants, such as selenate and cadmium are among the major constraints to crop productivity.

The plant open reading frames *MFS10*, *MFS11* and *MFS12* were expressed in yeast, exploiting this organism as a heterologous expression system. This eukaryote model offers several advantages, such as culture simplicity, rapid cell growth, low cost and the possibility of posttranslational modifications. Additionally, there are a huge amount of data, bioinformatic tools and biological material available to facilitate research in yeast.

The work described in this thesis is focused on the preliminary characterization of these three *A. thaliana* MFS transporters. To reach this goal, several abiotic stresses such as the effect of several cytotoxic compounds was examined. This research will help efforts on the characterization of the biological role of these plant transporters with expected impact in the development of efficient strategies of agricultural relevance.

The research performed involved the construction of recombinant plasmids to allow the expression of the three plant genes in yeast cells. The three cDNA sequences corresponding to the three ORFs were obtained at IGC and were cloned at IST into yeast expression vectors by homologous recombination. By phenotypical analysis, it was compared the level of susceptibility to several abiotic stresses of agricultural relevance of yeast cells expressing the plant genes. Sub-cellular localization assays were performed with yeast cells harboring the plasmid constructions to allow the expression of the GFP-fused proteins of interest.

## 2. Material and Methods

### 2.1. Yeast strains and growth conditions

The strain used in this study were the parental *S. cerevisiae* strain BY4741 (*MATa*, *his3Δ1*, *leu2Δ0*, *met15Δ0*, and *ura3Δ0*) and the derived deletion mutant BY4741\_Δ*qdr2* (*MATa*, *his3Δ1*, *leu2Δ0*, *met15Δ0*, *ura3Δ0*, *YIL121W::kanMX4*) obtained from the EUROSCARF collection. These strains were kept at -80°C in rich growth medium Yeast Peptone Dextrose (YPD) (described below) supplemented with 30% glycerol (v/v) (Merck). Fresh cultures were obtained by transferring a portion of the frozen cellular material to plates of solid YPD, followed by incubation at 30°C until visible cell growth.

Rich growth medium YPD used for yeast cell cultivation contains (per liter): 20 g glucose (Merck), 20 g yeast extract (Difco) and 10 g of bacto-peptone (Difco). Yeast cells harboring plasmids were cultivated in minimal growth medium MMB without uracil (MMB-U) at pH 4 or 4.5, containing (per liter): 1.7 g yeast nitrogen base without amino acids, 20 g glucose (supplemented or not with 0.1% of galactose) (Merck), 2.65 g (NH<sub>4</sub>)<sub>2</sub>SO<sub>4</sub> (Panreac), 20 mg L-histidine (Merck), 20 mg L-methionine (Sigma) and 60 mg L-leucine (Sigma). Solid medium was prepared by adding 20 g L<sup>-1</sup> agar (Iberagar) to MMB-U. Yeast growth was performed in MMB-U to assure plasmid maintenance in cells harboring pGREG576/pGREG596 or derived plasmids (Jansen *et al.*, 2005).

Yeast cells were also cultivated in ammonium phosphate medium (KNA) at pH 5.8 to perform K<sup>+</sup> limitation assays. The KNA medium contains (per liter): 0.492 g MgSO<sub>4</sub>·7H<sub>2</sub>O (Merck), 0.026 g anhydrous CaCl<sub>2</sub> (Panreac), 1.056 g (NH<sub>4</sub>)<sub>2</sub>HPO<sub>4</sub> (Merck), 3.96 g (NH<sub>4</sub>)<sub>2</sub>SO<sub>4</sub> (Panreac), 20 g glucose (Merck), 1 g galactose (Sigma); 10 mg L-histidine (Merck), 10 mg L-methionine (Merck), 10 mg L-leucine (Sigma), 2 mg Niacina (Sigma), 2 mg piridoxina (Sigma), 2 mg thiamine (Sigma), 2 mg D-panthothenic acid hemicalcium salt (Sigma), 0.02 mg biotin and the desired concentration of KCl: 0.2 mM (0.149 g L<sup>-1</sup>) or 2 mM (1.49 g L<sup>-1</sup>). Solid medium was prepared by adding 20 g L<sup>-1</sup> agar (Iberagar), and supplied or not with KCl to obtain final concentrations of 0 mM KCl, 0.2 mM KCl, 2 mM and 50 mM KCl.

### 2.2. Optimization of polymerase chain reaction conditions

The reaction mix to amplify by PCR the *MFS10*, *MFS11* and *MFS12* DNA sequences, in a final volume of 50 μL, was prepared as follows: 10 μL of 5xHF buffer, 1 μL dNTPs (10 mM), 2.5 μL of both "forward" and "reverse" primers (50 pmol. μL<sup>-1</sup>), 2 μL template DNA, 2 μL Mg<sup>2+</sup>, 0.5 μL of Phusion Taq polymerase and deionized H<sub>2</sub>O to complete to the specified final volume. All the used reagents belong to the Thermo Scientific® phusion HF PRC kit. The PCR conditions were programmed on a C1000 Thermal Cycler (BioRad) as follows: 30 sec at 98°C, then 30 cycles repeating the set of three steps: 10 sec at 98°C for denaturation, 20 sec at T<sub>m</sub>=56°C for annealing and 1 min at 72°C for extension, followed by 7 min additional extension at 72°C.

To optimize PCR amplification, different annealing temperatures were tested, between 52°C and 60°C. The concentration of Mg<sup>2+</sup> was tested in a range between 0.5 mM and 1 mM. The gene sequences

were amplified from cDNA generated from total *A. thaliana* seedlings RNA. The cDNA was supplied by our IGC collaborators. The designed primers contain nucleotide sequences with homology to the cloning site flanking regions of the pGREG576 and pGREG596 vector.

The resulting amplification products were separated by agarose gel electrophoresis (0.8% [w/v], SeaKem). A commercial DNA marker of 1 kb was also applied to the gel to allow subsequent identification of DNA fragments through their molecular weight. The gel was immersed in a GelRed™ (1000x, Biotium) 1x solution 20 minutes. This coloring agent intercalates the DNA molecules and fluoresces when exposed to ultraviolet light. PCR amplification fragments were purified using JETquick Gel Extraction spin kit from Genomed, according to the manufacturer instructions.

### **2.3. Cloning of *A. thaliana* *MFS10*, *MFS11* and *MFS12* genes in a yeast expression cloning vector**

#### **2.3.1. Drag & Drop cloning method**

The Drag&Drop strategy was used to clone and express the *A. thaliana* *MFS10*, *MFS11* and *MFS12* in *S. cerevisiae* (Jansen *et al.*, 2005). This technique uses *in vivo* homologous recombination to insert genes of interest into galactose-inducible expression vectors (pGREGs), leading to the formation of amino-terminal fusions. All the vectors contain common regions for recombination that flank the stuffer fragment (*rec1* and *rec2*). The introduction of common recombination sequences at the end of PCR fragments allows the cloning of genes without the need of specific restriction sites. In this process, the selectable stuffer *HIS3* gene is replaced by successful gene integration, and a screen for loss of the selection marker identifies potential recombinants (loss of the capability to grow in a medium without histidine). This strategy leads to specific fusion proteins (amino-terminal fusions between the gene of interest and different tags) (figure 2.1).

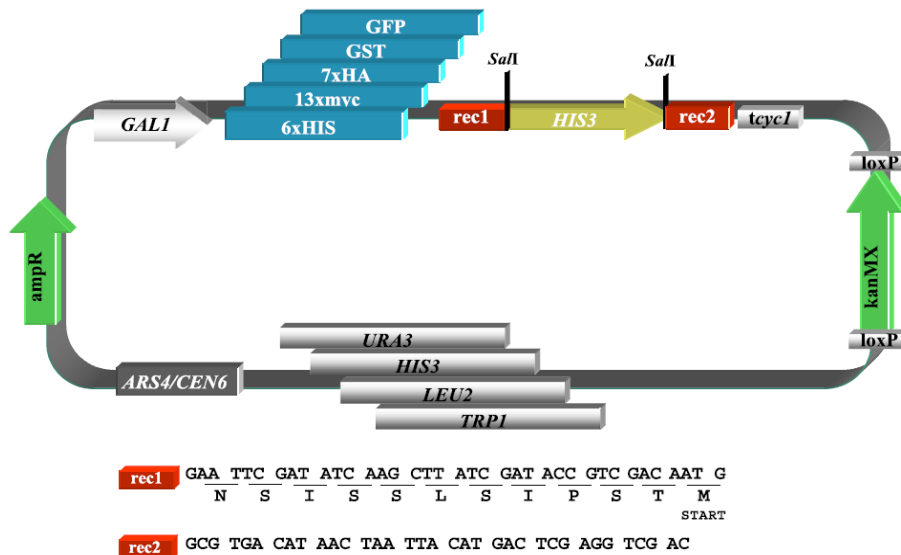


**Figure 2.1 – Schematic representation of the basic pGREG vector system.** The inducible GAL1 promoter controls the expression of tags or generated fusion proteins. Downstream of the tags a *HIS3* stuffer fragment is flanked by specific sites for recombination, *rec1* and *rec2*. The vectors contain one of the selectable yeast markers *URA3*, *LEU2*, *TRP1* and *HIS3*, the selectable *E. coli* marker *ampR* (ampicillin resistance), as well as an additional KanMX cassette flanked by *loxP* sites. Sequences of *rec1* and *rec2* used for the targeted *in vivo* recombination of DNA fragments into the vector, including the translated sequence encoded by the *rec1* linker between the tag and the protein of interest (Jansen *et al.*, 2005).

The pGREG576 and pGREG596 plasmid from the Drag&Drop collection (Jansen *et al.*, 2005) were chosen to clone and express the *MFS10*, *MFS11* and *MFS12* genes in yeast cells. These plasmids were acquired from EUROSCARF and contain a galactose inducible promoter (GAL1), the yeast selectable marker *URA3*, and the *GFP* tag sequence. The *GFP* tag encodes a green fluorescent protein (GFPS65T), which allows monitoring of the expression and sub-cellular localization of the cloned fusion protein. These plasmids are similar but, in pGREG596, a myristoylation sequence is present linked to the NH2 terminus of GFP (Jansen *et al.* 2005) (figure 2.2).

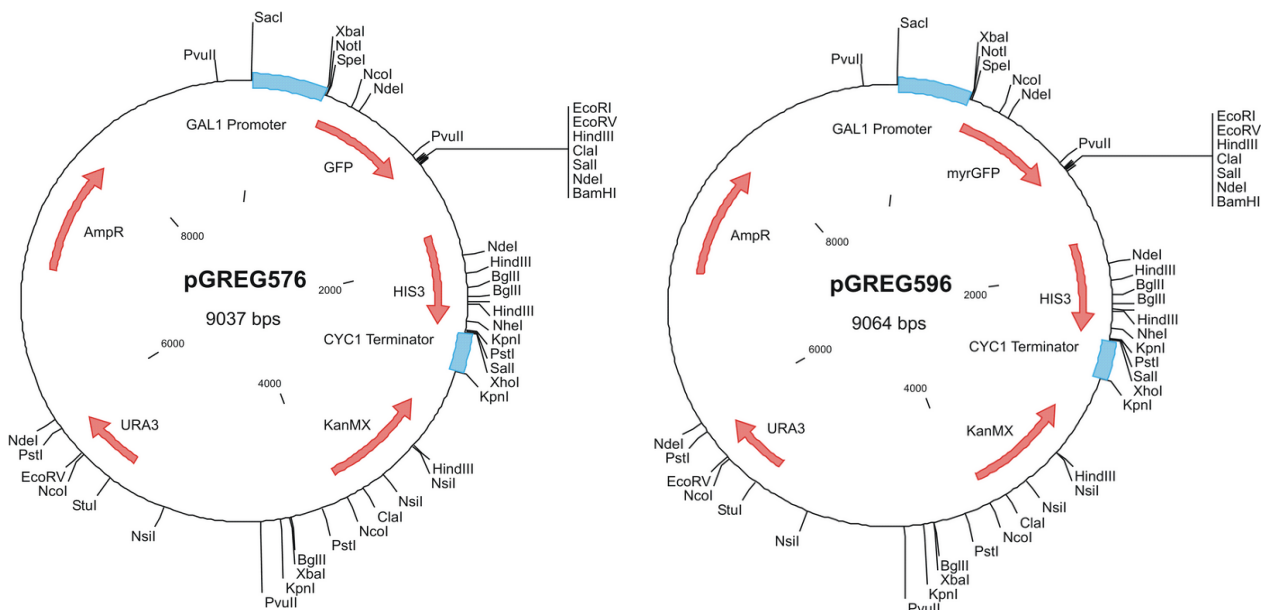


**Figure 2.2 - Schematic representation of the pGREG576 and pGREG596 vector.** The restriction sites and respective enzymes are also indicated (EUROSCARF).

After PCR amplification, the three plant sequences became flanked by short sequences with homologies to the vector. Each PCR fragment was co-transformed into a *S. cerevisiae* strain with the pGREG576 or pGREG596 vector previously cut with *SalI* restriction enzyme (figure 2.3).

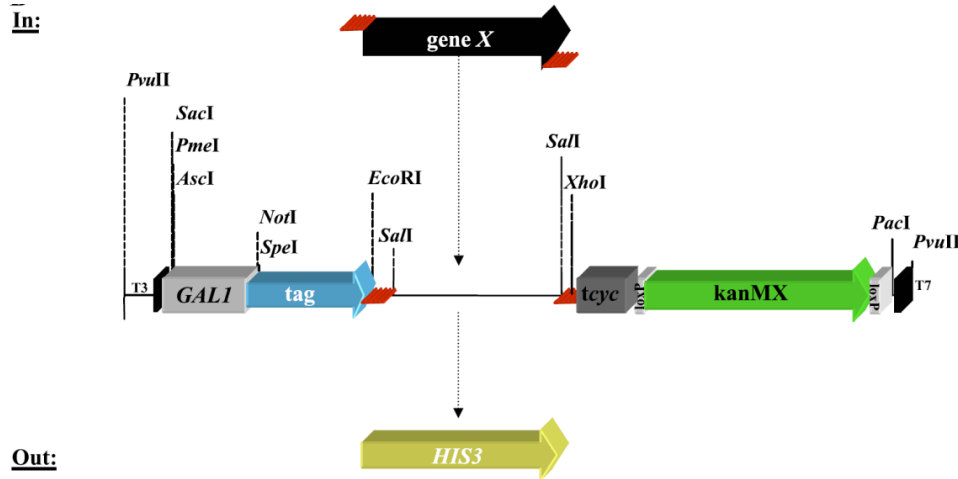


**Figure 2.3 - Targeted recombination into pGREG vectors.** First the cloning vector is cut with *SalI*, which leads to the removal of the *HIS3* stuffer fragment. Then the gene *X* (*MFS10*, *MFS11* or *MFS12*), flanked by *rec1* and *rec2*, successfully integrates the vector by homologous recombination (Jansen et al., 2005).

### 2.3.2. pGREG576/ pGREG596 restriction

The restriction of the pGREG vectors with *SalI* restriction enzyme was executed in a total volume of 50 mL: 1 enzyme unity (1 U) for each 500 ng $\mu$ L<sup>-1</sup> of DNA and 5  $\mu$ L of react 10 enzyme buffer 10x (Invitrogen), and incubated at 37°C over-night (optimal enzyme temperature). Afterwards, 1.5 mL of calf intestinal alkaline phosphatase (CIAP, Invitrogen) were added and the mixture was kept at 37°C for 45 min. This phosphatase catalyzes the removal of 5' phosphate groups from DNA. Therefore, the two blunt ends of the cut vector cannot self-ligate, increasing homologous recombination probability. The restriction product was directly used in yeast transformation.

### 2.3.3. Yeast transformation

The BY4741 yeast cells suspension was grown in 50 mL of YPD, at 30°C with orbital agitation (250 rpm), until a standardized culture OD<sub>600</sub> between 0.5 – 0.7. 50 mL of cell culture was centrifuged (5 minutes, 6000 rpm, 4°C) twice, being resuspended successively in 4.5 mL of TE buffer (Alkali-Cation™ Yeast Kit) and 2.5 mL Lithium/Cesium acetate solution (Alkali-Cation™ Yeast Kit), respectively. Cells were incubated for 25 minutes at 30°C with gentle orbital agitation (100 rpm) and centrifuged (same conditions), followed by resuspension on 500  $\mu$ L TE buffer. Cells were then ready for transformation using Alkali-Cation™ Yeast Kit following manufacturer instructions plated and incubated at 30°C for 48 hours. The transformants were plated onto selective medium, without uracil, MMB-U. After growth, the transformants were patched onto fresh plates.

#### **2.3.4. Vector construction confirmation**

The recombinant plasmids pGREG576\_MFS10, pGREG576\_MFS11 and pGREG576\_MFS12 were obtained through homologous recombination in yeast, by replacement of the *HIS3* fragment. Since plasmid DNA cannot be efficiently extracted from yeast cells, the strategy used implicated total DNA extraction from yeast cells and *E. coli* transformation with the DNA solution obtained. Once transferred to *E. coli*, plasmid DNA can be efficiently extracted from bacterial cells.

#### **2.3.5. Yeast total DNA extraction**

Adequate amounts of cell culture from the selected clones were resuspended in 200 mL of desionized water. The cellular lysis was accomplished using an equal volume of glass beads (425-600 mm of diameter, Sigma). 300 mL of a phenol/chloroform/isoamlic acid mixture (25:24:1 proportion, AMRESCO) were added, followed by a 2 min vortex. The mixtures were centrifuged (14000 rpm, 5 min) and the supernatants subjected to another phenol extraction. The final supernatants were then subjected to an ether extraction (300 mL). DNA was purified by ethanol 100% (Riedel-de-Haen) precipitation (900 mL) and incubated at -20°C for about 15 min. The tubes were then centrifuged (15000 rpm, 4°C, 15 min), the formed precipitate washed with 500 mL of ethanol 70% (v/v) and dried in vacuum for about 10 min. The total DNA was dissolved in 30 mL of sterile water and stored at -20°C until further use. A confirmation PCR was done in order to confirm the presence of the desired genes in the plasmid constructions, using the pGREG universal primers: 5' - GCTTATCGATACCGTCGACA-3' and 5' - TTACATGACTCGAGGTGAC – 3'.

#### **2.3.6. E. coli electroporation**

##### Electrocompetent cell preparation

The *E. coli* strain used for vector container was the XL1-Blue. A cell suspension was grown in 100 mL of Lurian-Bertani Broth (LB) medium that contains (per litre): 20 g of LB broth (Conda), at 37°C with orbital agitation (250 rpm), until a standardized culture OD640nm of about 0.8. The pellet obtained from centrifugation (8000 rpm, 4°C, 15 min) was successively washed with sterile water. The resultant pellet was resuspended in 4 mL of sterile glycerol 10% (v/v) (Merck) and centrifuged (8000 rpm, 4°C, 15 min). Finally, the cells were resuspended in 2 mL of glycerol 10%, divided into 110 mL aliquots and stored at -80°C until further use.

##### Electroporation

Electrocompetent *E. coli* cells were unfreezed on ice. Electrocompetent cells were mix with 10 µl of total DNA extracted from yeast cells and transferred to a cold and sterile electrotransformation cuvette (electrode distance: 0.2 cm) and subjected to an electric pulse of 2.5 V (Gene Pulser™, Biorad). LB was added to promote cell regeneration after the shock (incubation for 1h at 37°C with orbital agitation, 250 rpm). Later, the cells were plated in LB solid medium supplemented with ampicillin. The *E. coli* cells successful transformed with pGREG plasmids are able to growth in the presence of ampicillin due to the selectable marker ampR expressed in *E. coli* from the pGREG plasmids.

### **2.3.7. Plasmid DNA extraction**

Plasmid DNA was extracted using the alkaline lysis method. Each colony was grown in 3 mL of LB supplemented with ampicillin at 37°C with orbital agitation (250 rpm) overnight. Then, the cellular suspensions were centrifuged (14000 rpm, 2 min) and the obtained pellets resuspended in 150 mL of solution I (50 mM glucose (Merck) 10 mM EDTA (Aldrich), 25 mM Tris-HCl pH 8.0 (Sigma), 10 mg/mL lysozyme (Sigma)). The Tris-HCl in this solution causes chelation of  $Mg^{2+}$  and  $Ca^{2+}$ . The lysozyme promotes cellular lysis. The mixtures were kept for 5 min at room temperature. Following it was added 200 mL of solution II to each sample and kept in ice for 5 min. Solution II was only prepared at the time of the experiment by mixture of the denaturant agents SDS 10% (w/v) (Sigma) and 2 M NaOH (Merck) in deionized water. Finally, genomic DNA precipitation was carried out by addition of 150 mL of solution III (5 M potassium acetate (Merck), acetic acid 11.8% (v/v)), which contains a potassium salt that partially precipitates the SDS molecules attached to the proteins in the supernatant. The cellular suspensions were kept in ice for 10 min and then centrifuged (14000, 15 min). The supernatants were transferred to new eppendorfs with 900 mL of ethanol 100% (Riedel-de-Haën) and incubated at -20°C for 30 min. The formed precipitates were washed with 500 mL of ethanol 70% (v/v) and dried in vacuum 10 min. The DNA was dissolved in 30 mL of sterile water. For higher purity level such DNA sequencing, the plasmid DNA was extracted using QIAprep® Spin Miniprep kit (Qiagen), according to the manufacturer instructions.

### **2.3.8. Plasmid DNA restriction profile**

Plasmid DNA was extracted from transformed *E. coli* cells using the alkaline lysis method. Restriction patterns were used to check if the DNA extracted corresponds to the correct construction. Plasmid constructions have different restriction patterns according to recirculation of the cloning vector or a successful homologous recombination with the desired genes. To choose a restriction enzyme, the restriction maps of pGREG596\_MFS10, pGREG596\_MFS11, pGREG576\_MFS10, pGREG576\_MFS11 and pGREG576\_MFS12 plasmids were analyzed. This analysis was performed through the bioinformatic tool “Yeast Genome Restriction Analysis” ([www.yeastgenome.org/cgi-bin/PATMATCH/RestrictionMapper](http://www.yeastgenome.org/cgi-bin/PATMATCH/RestrictionMapper)). These reactions were carried out by addition of 1 U for each 500 ng $\mu$ L<sup>-1</sup> of DNA in a total volume of 30 mL, with suppliers indicated concentration of the enzyme buffer. The reaction mixtures were incubated at 37°C (optimal temperature for the used enzymes) for at least 2h. The resulting DNA fragments were separated by agarose gel electrophoresis (0.7% (w/v), SeaKem®). A commercial DNA marker of 1 kb was also applied to the gel, which allows subsequent identification of the molecular weight of DNA fragments.

### 2.3.9. Plasmid DNA sequencing

Two positive candidates of each derivative plasmid were chosen and the plasmid DNA of these candidates were extracted with QuiaPrep<sup>®</sup> Spin Miniprep kit and order to sequence with the previously mentioned pGREG universal primers. The middle part of the MFS10 gene was sequenced using a custom made primer. All sequencing work was performed by STABvida.

### 2.4. Sub-cellular GFP-fused protein localization

The sub-cellular localization of the MFS10-GFP, MFS11-GFP and MFS12-GFP fusion proteins was assessed by fluorescence microscopy after protein induction. The cell culture was prepared by suspension in MMB-U liquid medium supplemented or not with 0.5% galactose. The cell suspension was grown at 30°C with orbital agitation (250 rpm), until the standardized culture  $OD_{600nm} = 0.4 \pm 0.04$  was reached. At this point, cells suspension without galactose were filtered and moved to MMB-U liquid medium with 1% or 2% galactose and without glucose or it was added a pulse of 2% galactose to the inoculum medium. The cultivation media were incubated at 30°C with orbital agitation (250 rpm), until the standardized culture  $OD_{600nm} = 0.4 \pm 0.04$  was reached. The sub-cellular localization of MFS10-GFP, MFS11-GFP and MFS12-GFP fusion proteins in *S. cerevisiae* living cells was observed upon 1.5-3 h of incubation of the yeast cells harboring the pGREG plasmid construction in the presence of galactose by fluorescence microscopy in a Zeiss Axioplan microscope (Carl Zeiss MicroImaging), using excitation and emission wavelengths of 395 and 509 nm, respectively. Observations were performed during a period of 10 h and after around 24 hours.

### 2.5. Chemical stress susceptibility plate assays

The susceptibility of the parental strain BY4741 or the mutant strain  $\Delta qdr2$  harboring the empty cloning vector pGREG596 or pGREG597 or the derived plasmids pGREG596\_ *MFS10*, pGREG596\_ *MFS11*, pGREG576\_ *MFS10*, pGREG576\_ *MFS11* or pGREG576\_ *MFS12* was assessed by spot assays.

For chemical stress susceptibility assays, cell suspensions were prepared by cultivation in liquid MMB-U media (supplemented with 0.1% of galactose), at 30°C with orbital agitation (250 rpm), until the standardized culture  $OD_{600nm} = 0.3 \pm 0.02$  was reached, followed by dilution to a standardized  $OD_{600nm} = 0.05 \pm 0.005$ . These cell suspensions and subsequent dilutions (1:5 and 1:25) were applied as spots (4 $\mu$ L) onto the surface of the agarized MMB-U media (supplemented with 0.1% of galactose to induce moderate gene expression), pH 4.5 (adjusted with HCl), supplemented with inhibitory concentrations of the chemical stress inducers tested. For iron deprivation assays yeast nitrogen base lacking iron was used to prepare the agarized media. Plates were incubated at 30°C for 3–8 days, depending on the severity of growth inhibition. The tested metals and other compounds were used in different concentration ranges and are described in table 2.2. Pesticides and indole-3-acetic acid were obtained from Sigma and dissolved in dimethyl sulfoxide (DMSO Sigma). The solvent used was added to the control plates at the maximum concentration used for toxicity assays. The remaining compounds were obtained from Sigma or Merck and were dissolved in deionised sterile water.

**Table 2.1 – Range of concentrations of the tested compounds in chemical stress susceptibility assays with yeast cells harboring pGREG596\_MFS10, pGREG596\_MFS11, pGREG576\_MFS10, pGREG576\_MFS11 or pGREG576\_MFS12.**

Tested compounds	Range of concentration (mM)
Aluminum sulphate hexadecahydrate ( $\text{Al}_2\text{O}_{12}\text{S}_3 \cdot 16\text{H}_2\text{O}$ )	2 – 5
Cadmium chloride hemi (penta-hydrate) ( $\text{CdCl}_2 \cdot 2,5\text{H}_2\text{O}$ )	0.02 – 0.12
Cesium chloride ( $\text{CsCl}_2$ )	15 – 25
Copper chloride dihydrate ( $\text{CuCl}_2 \cdot 2\text{H}_2\text{O}$ )	0.5 – 3
Cobalt (II) sulfat-heptahydrate ( $\text{CoSO}_4 \cdot 7\text{H}_2\text{O}$ )	1 – 2
Iron (III) chloride hexahydrate ( $\text{FeCl}_3 \cdot 6\text{H}_2\text{O}$ )*	0.1 - 2
Lead chloride ( $\text{PbCl}_2$ )	1.5 – 3.5
Manganese chloride dehydrate ( $\text{MnCl}_2 \cdot 4\text{H}_2\text{O}$ )	15 – 36
Nickel Sulphate ( $\text{NiSO}_4 \cdot 6\text{H}_2\text{O}$ )	0.5 – 1.6
Sodium chloride ( $\text{NaCl}_2$ )	600 - 2000
Thallium (III) chloride tetrahydrate ( $\text{TlCl}_3 \cdot \text{H}_2\text{O}$ )	0.5 – 1
Zinc chloride ( $\text{ZnCl}_2$ )	20 – 35
2,4-dichlorophenoxyacetic acid sodium salt mono hydrate ( $\text{C}_8\text{H}_6\text{Cl}_2\text{O}_3$ )	1.5 – 6
2-methyl-4-chlorophenoxyacetic acid sodium ( $\text{C}_9\text{H}_8\text{ClO}_3\text{Na}$ )	0.25 – 1.5
2,4-Dichlorophenol ( $\text{C}_6\text{H}_4\text{Cl}_2\text{O}$ )	0.5 – 2.5
indole-3-acetic acid ( $\text{C}_{10}\text{H}_8\text{NNaO}_2$ )	0.05 – 0.15
Acetic Acid ( $\text{CH}_3\text{COOH}$ )	60 - 70
L-Malic Acid ( $\text{C}_4\text{H}_6\text{O}_5$ )	130 - 160
Citric Acid ( $\text{C}_6\text{H}_8\text{O}_7$ )	60 - 70
Succinic acid ( $\text{C}_4\text{H}_6\text{O}_4$ )	150 - 170
Alachlor ( $\text{C}_{14}\text{H}_2\text{ClNO}_2$ )	100 – 400 mg/L
Metolachlor ( $\text{C}_{15}\text{H}_{22}\text{ClNO}_2$ )	100 – 500 mg/L
D-Mannitol ( $\text{C}_6\text{H}_{14}\text{O}_6$ )**	400 - 1850

\*exclusively for yeast cells harboring pGREG576\_MFS12

\*\*exclusively for yeast cells harboring pGREG576\_MFS10 or pGREG596\_MFS10

## 3. Results

### 3.1. *A. thaliana* cDNA amplification and plasmid construction

The pGREG576 and pGREG596 plasmids from the Drag and Drop collection (Jansen *et al.*, 2005) were used to clone and express the *A. thaliana* ORFs *MFS10*, *MFS11* and *MFS12* in *S. cerevisiae*.

#### 3.1.1. Preparation of genetic constructions in pGREG576 plasmid

Amplification of the *MFS10*, *MFS11* and *MFS12* fragments for recombinant plasmid construction was achieved using the appropriate primers and plant cDNA as template. The cDNA was generated from RNA extracted from *A. thaliana* seedlings in the Plant Molecular Biology Group of Instituto Gulbenkian de Ciência. The designed primers contain a nucleotide sequences with homology to the start and end coding region of the *MFS10*, *MFS11* or *MFS12* fragments, and other fraction with homology to the cloning site flanking regions of the pGREG576 vector.

The first attempt for *MFS10* sequence amplification failed due to absence or low *MFS10* cDNA in the sample received from IGC partners. Its amplification was subsequently possible following the supply of a new cDNA sample, generated from RNA extracted from *A. thaliana* seedlings exposed to salt stress. With the exception of the annealing temperature, the PCR conditions remained the same in the PCR amplifications performed. The annealing temperature for *MFS10* and *MFS11* amplification was 56°C but the *MFS12* amplification temperature had to be optimized, since at an annealing temperature of 56°C there was no amplification. The annealing temperature found to allow *MFS12* PCR amplification was 52°C. The PCR products analysis by gel electrophoresis confirmed the expected size of the amplified fragments *MFS10*, *MFS11* and *MFS12* of 1686 bp, 1370 bp and 1572 bp, respectively (figure 3.1). The fragments of expected size were extracted from the gel and used for the next steps.

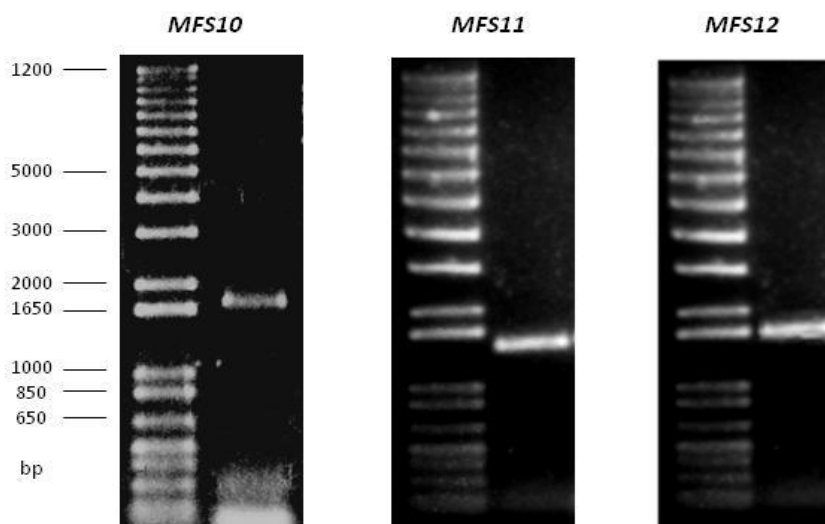


Figure 3.1 – *MFS10* fragment (1686 bp), *MFS11* fragment (1370 bp) and *MFS12* (1572 bp) fragment PCR amplification.

The recombinant plasmids pGREG576\_*MFS10*, pGREG576\_*MFS11* and pGREG576\_*MFS12* were obtained through homologous recombination in yeast. The *HIS3* fragment was replaced by *MFS10*, *MFS11* or *MFS12* fragments (figures 2.2 and 2.3, in material and methods). The plasmid constructions were first confirmed by enzyme restriction profile. The restriction map predicted with *HindIII* generated four or three fragments for each plasmid, as described in the following table.

**Table 3.1 – Fragment sizes generated by pGREG576\_*MFS10*, pGREG576\_*MFS11* and pGREG576\_*MFS12* with *HindIII* (“Yeast Genome Restriction Analysis”: [www.yeastgenome.org/cgi-bin/PATMATCH/RestrictionMapper](http://www.yeastgenome.org/cgi-bin/PATMATCH/RestrictionMapper)).**

pGREG576_ <i>MFS10</i>	pGREG576_ <i>MFS11</i>	pGREG576_ <i>MFS12</i>
7027 bp	7027 bp	7027 bp
1262 bp	1235 bp	1483 bp
1088 bp	977 bp	931 bp
179 bp		

After enzyme restriction, the predicted fragment profiles were obtained (figure 3.2). Subsequent sequencing analysis of the pGREG576\_*MFS10*, pGREG576\_*MFS11* and pGREG576\_*MFS12* DNA inserts confirmed that the three correct gene sequences had been cloned.

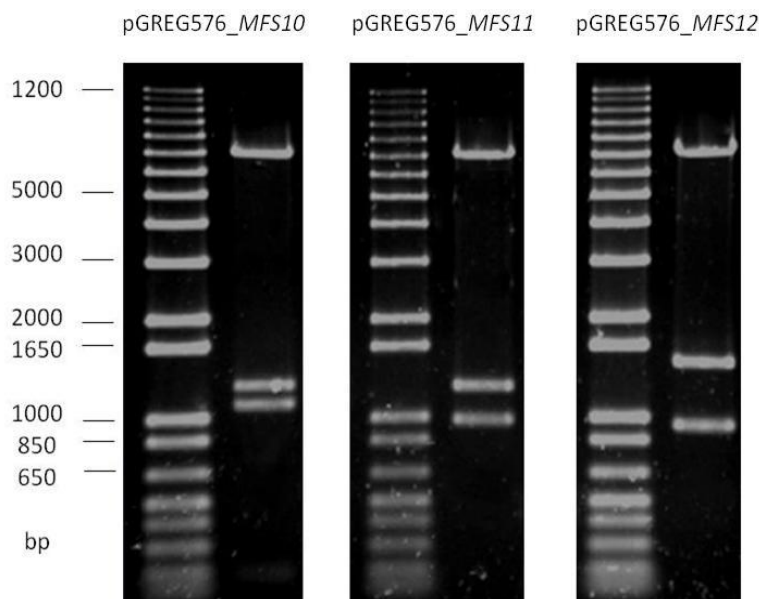


**Figure 3.2 – *HindIII* restriction profile of the plasmid constructions pGREG576\_*MFS10*, pGREG576\_*MFS11* and pGREG576\_*MFS12*.**

### 3.1.2. Preparation of genetic constructions in pGREG596 plasmid

In an attempt to optimize the functional heterologous expression of the plant transporters in yeast, the pGREG596 plasmid was also used to clone the *A. thaliana* ORFs and express them in *S. cerevisiae*. When compared with the vector pGREG576, the vector pGREG596 contains a myrGFP amino-terminal tag, to be fused to the GFP fused-membrane transporter, which is a plasma membrane localization signal (figure 2.2, in material and methods). Therefore, the plant transporters when cloned in this vector are supposed to be targeted to the plasma membrane. The plasmid construction strategy

followed the same steps as described above. But the previous constructions prepared were used as template for amplification of *MFS10*, *MFS11* and *MFS12* fragments. The primers and PCR conditions used were the same as before (figure 3.3).

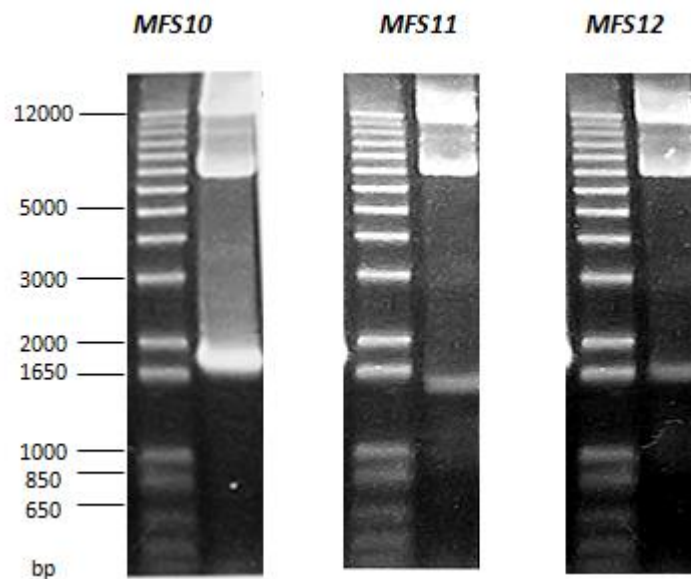


Figure 3.3 – *MFS10* fragment (1686 bp), *MFS11* fragment (1370 bp) and *MFS12* (1572 bp) fragment PCR amplification.

After homologous recombination, the constructions were confirmed by enzyme restriction. Plasmids pGREG596 and pGREG576 constructions have the same *HindIII* restriction sites. Given this, the restriction map predicted with *HindIII* also provided four fragments for pGREG596\_*MFS10* and three fragments for pGREG596\_*MFS11* and pGREG596\_*MFS12* ([www.yeastgenome.org/cgi-bin/PATMATCH/RestrictionMapper](http://www.yeastgenome.org/cgi-bin/PATMATCH/RestrictionMapper)) (table 3.1). The figure 3.4 shows the confirmed restriction profiles after restriction.

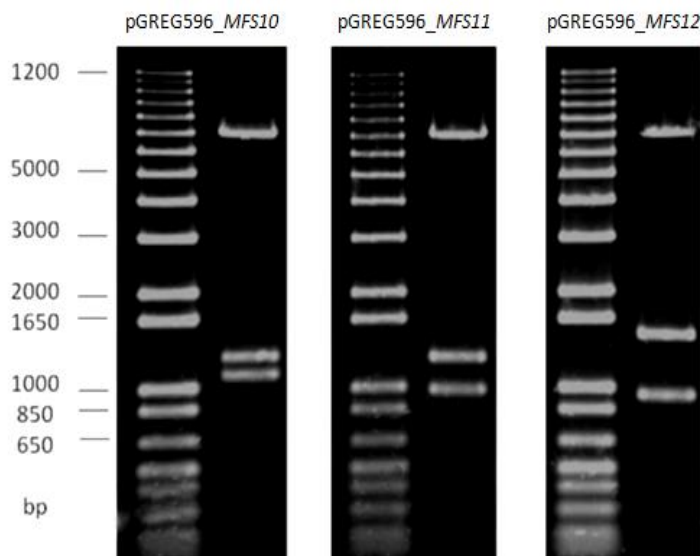
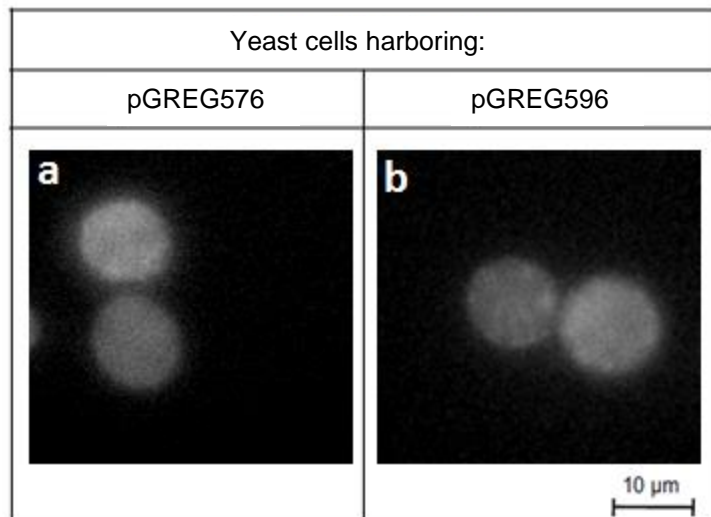


Figure 3.4 – *HindIII* restriction profile of plasmid constructions pGREG596\_*MFS10*, pGREG596\_*MFS11* and pGREG596\_*MFS12*.

Subsequent sequencing analysis of the pGREG596\_ *MFS10* and pGREG596\_ *MFS11* confirmed the correct cloning of *MFS10* and *MFS11* genes, but not in the one of pGREG596\_ *MFS12* inserted. Therefore, only the yeast cells harboring pGREG596\_ *MFS10* or pGREG596\_ *MFS11* were examined at the fluorescence microscope.

### 3.2. Sub-cellular localization assays

Yeast cells either expressing the plant genes (pGREG576\_ *MFS10*, pGREG576\_ *MFS11* pGREG576\_ *MFS12*; pGREG596\_ *MFS10* and pGREG596\_ *MFS11*) or harboring the empty cloning vectors pGREGE576 or pGREGE596, were cultivated in medium containing 2% galactose as the sole carbon source to allow full induction of the plant gene under the control of *GAL1* promoter. Control cells harboring the empty cloning vectors pGREGE576 or pGREGE596 showed a weak and uniform distribution of green fluorescence all over the cell, due to basal fluorescence (figure 3.5).



**Figure 3.5 – Fluorescence microscopy images of exponential-phase BY4741 cells harboring the empty vector pGREG576 (a) or pGREG596 (b).**

#### 3.2.1. *MFS10* – GFP fusion protein sub-cellular localization

The yeast cells harboring plasmid pGREG576\_ *MFS10* showed fluorescent dots throughout the cell, following galactose-induced GFP-fused protein production (figure 3.6a). The number and the fluorescence intensity of these dots increased over time. Thus, it was assessed the localization of *MFS-10* GFP fusion protein from BY4741\_pGREG596\_ *MFS10* cells in an effort to achieve a plasma membrane localization. However, even under such conditions the localization of *MFS10* was not completely clear. After 2.5 h of galactose induction, it was observed fluorescence in general associated to cell periphery potentially to plasma membrane. However, fluorescence localization was not uniformly distributed at the plasma membrane but was observed as spots in specific regions all over the cell periphery (figure 3.6b). Over time, fluorescence spread throughout the cell.

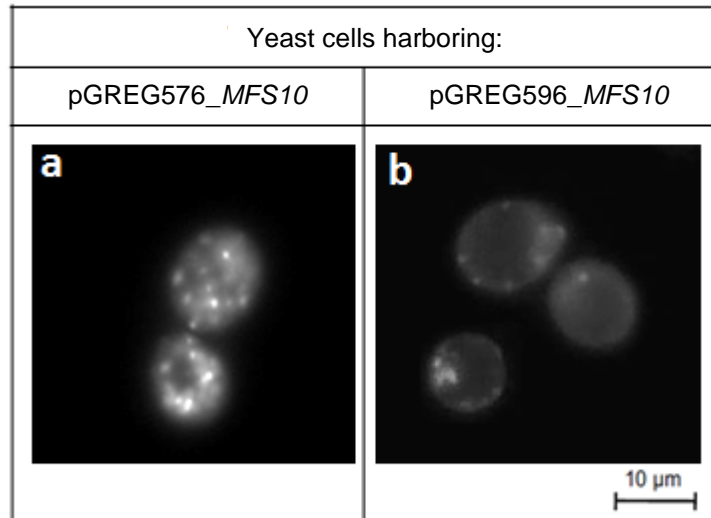


Figure 3.6 – Fluorescence microscopy images of exponential-phase BY4741 cells harboring the plasmid pGREG576\_*MFS10* (a) or pGREG596\_*MFS10* (b) after 2.5 h of galactose-induced GFP-fused protein production.

### 3.2.2. *MFS11* – GFP fusion protein sub-cellular localization

Yeast cells harboring plasmid pGREG576\_*MFS11* showed fluorescent dots throughout the cytosol, but in general close to the periphery (figure 3.7a). The number and fluorescence level of these dots tend to increase over time. However, due to the absence of a clear plasma membrane localization, the localization of *MFS-11* GFP fusion protein from yeast cells harboring pGREG596\_*MFS11* was assessed. Yeast cells expressing plasmid pGREG596\_*MFS11* showed small dots apparently localized at the plasma membrane, after 1.5 hour of galactose induction. Over time, these dots remained associated to cell periphery, although increasing their size (Figure 3.7b). Similar to BY4741\_pGREG596\_*MFS10*, the resulted pattern may suggest that the fluorescent-fused protein is partially localized at the plasma membrane.

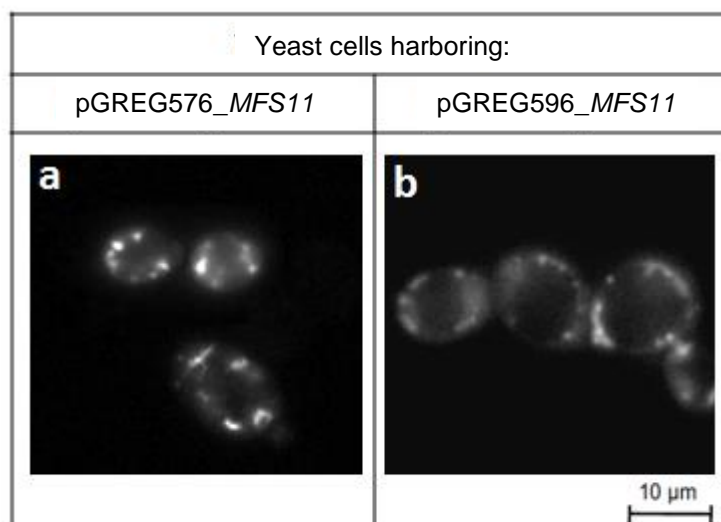
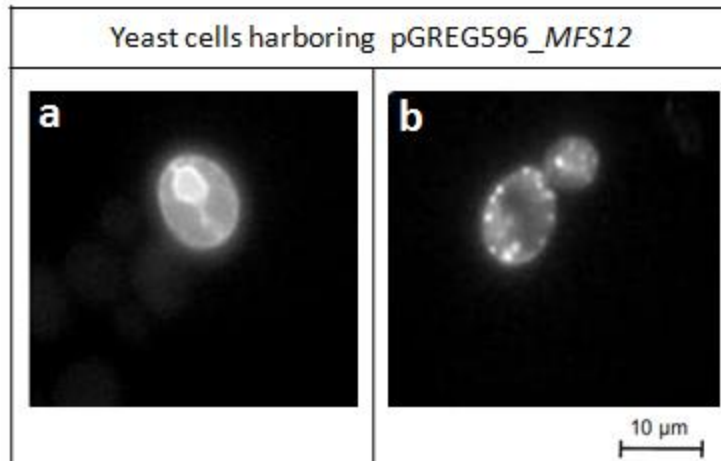


Figure 3.7 – Fluorescence microscopy images of exponential-phase BY4741 cells harboring the plasmid pGREG576\_*MFS11* after 2.5 h of galactose-induced GFP-fused-protein production (a) or the plasmid pGREG596\_*MFS11* after 1.5 h of galactose-induced GFP-fused-protein protein production (b).

### 3.2.3. MFS12 – GFP fusion protein sub-cellular localization

MFS12-GFP fusion protein was only observed in yeast cells expressing the pGREG576 construction because no alternative localization could be constructed obtained. After 2.5 h of galactose-induction, MFS12-GFP fusion protein localized at plasma membrane and showed also an internal membrane localization, presumably at endoplasmic reticulum membrane (figure 3.8a). After 3h of induction, a number of fluorescent dots were observed throughout the cell (figure 3.8b), similarly to what has been observed in yeast cells harboring pGREG576\_ *MFS10* or pGREG576\_ *MFS11*.



**Figure 3.8 – Fluorescence microscopy images of exponential-phase BY4741 cells harboring plasmid pGREG576\_ *MFS12* after 2.5 h of galactose-induced GFP-fused-protein production (a) and 3 h of galactose-induced GFP-fused-protein protein production (b).**

For all the constructions with the three plant gene inserted, the GFP fusion encoded proteins were observed in cell grown for period of 10 hours and after 24 hours of galactose induction. An increased fluorescence level and aggregation of fluorescent dots was observed over the incubation time, even 10 or 24 hours later. The attempt to vary the galactose concentration (0.5%, 1% and 2%) in the medium used to induce the GFP fused protein did not influence the results obtained.

### 3.3. Chemical stress susceptibility assays

Metals are important environmental pollutants exhibiting high toxicity towards plants when in toxic concentrations. To study the role of the expression of plant genes *MFS10*, *MFS11* and *MFS12* in yeast tolerance to metal ions, susceptibility spot assays were carried out. Yeast cells harboring the empty cloning vector or the plasmids pGREG576\_*MFS10*, pGREG576\_*MFS11* or pGREG576\_*MFS12* were examined in the same basal medium supplemented with different cytotoxic compounds.

The homology of *MFS10* with *ZIF2*, which is related to zinc tolerance led us test the tolerance of yeast cells expressing *MFS10*, *MFS11* or *MFS12* to  $Zn^{2+}$ . However, the expression of the plant genes in yeast cells did not confer either increased resistance or susceptibility to  $Zn^{2+}$  (data not shown).

As mentioned previously, microarray data in the literature appear to suggest up-regulation of *MFS10* transcripts in *A. thaliana* seedlings exposed to cadmium stress and the up-regulation of *MFS11* transcripts in *A. thaliana* seedlings exposed to salt stress (Zimmermann *et al.*, 2004). However, the expression of *MFS10*, *MFS11* or *MFS12* in yeast cell exposed to toxic concentrations of  $Cd^{2+}$  or salt did not affect their growth under these stresses (data not shown). Microarray data also indicate an up-regulation of *MFS12* transcripts in *A. thaliana* roots exposed to iron deprivation (Zimmermann *et al.*, 2004). When expressed in yeast cells exposed to iron deprivation, the *MFS12* gene apparently did not confer increased resistance or susceptibility to yeast cells exposed to iron limitation (data not shown).

*MFS11* has homology with *A. thaliana* gene *ZIFL1*. *ZIFL1.3* isoform expression in yeast cells was found to confer resistance to  $Al^{3+}$  and  $Ti^{3+}$  (Cabrito *et al.*, 2009). However, the expression of *MFS11* in yeast cells did not show any phenotype related to  $Al^{3+}$  and  $Ti^{3+}$  resistance and the same was found for *MFS12* expression (data not shown). However in yeast cells expressing *MFS10*, a subtle growth inhibition was registered in the presence of  $Al^{3+}$ , when compared with yeast cells harboring the empty cloning vector. This result suggests that *MFS10* expression confers, apparently, a higher susceptibility to  $Al^{3+}$  (figure 3.9). The expression of this plant gene did not result either in increased yeast resistance or susceptibility to  $Ti^{3+}$  (data not shown).

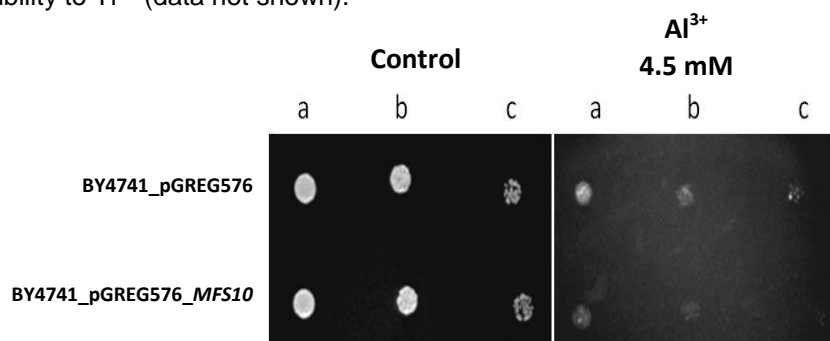
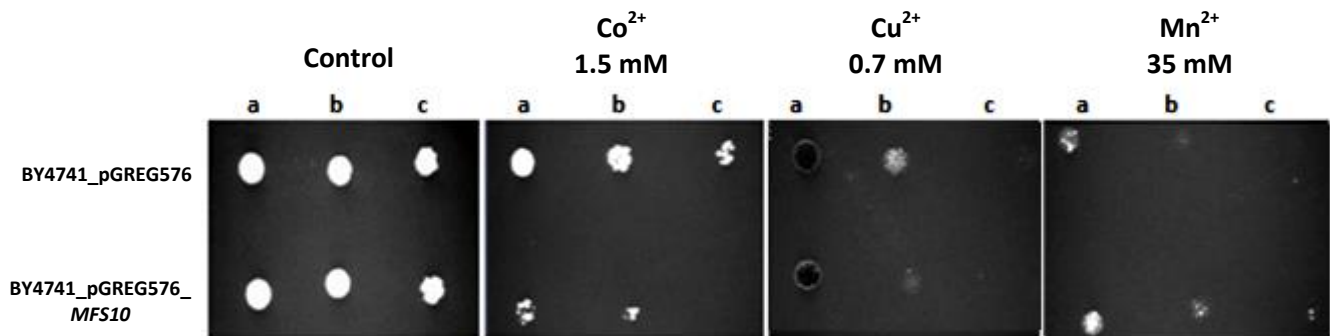
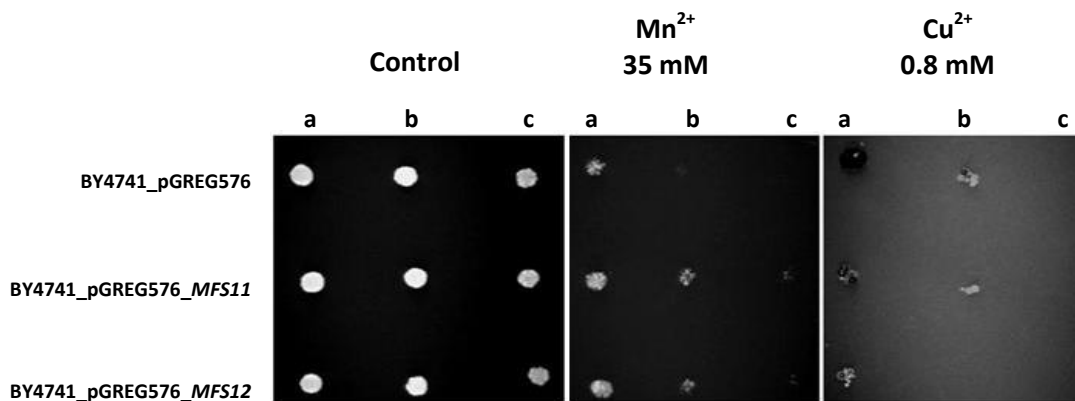


Figure 3.9 - Effect of the expression of *MFS10* in yeast cells exposed to  $Al^{3+}$  (4.5 mM). Cell suspensions used to prepare the spots were 1:5 (b) and 1:10 (c) dilutions of the cell suspension used in a. These pictures are representative of the results obtained in 3 replicates.

Other ion compounds were also examined, such as,  $\text{Cs}^+$ ,  $\text{Co}^{2+}$ ,  $\text{Cu}^{2+}$ ,  $\text{Mn}^{2+}$ ,  $\text{Pb}^{2+}$ ,  $\text{Ni}^+$  and  $\text{Na}^+$ . Apparently none of the plant genes conferred yeast resistance or susceptibility to  $\text{Ni}^+$  and  $\text{Pb}^{2+}$  (data not shown). *MFS10* gene expression conferred increased yeast susceptibility to  $\text{Co}^{2+}$  (figure 3.10), while *MFS11* or *MFS12* expression had no detectable effect in yeast cells exposed to this metal (data not shown). The expression of *MFS10*, *MFS11* or *MFS12* in yeast cells conferred increased resistance to  $\text{Mn}^{2+}$  (figure 3.10 and figure 3.11). Moreover, yeast cells expressing *MFS10* or *MFS12* were more susceptible to  $\text{Cu}^{2+}$ , when compared to yeast cells harboring the empty cloning vector, while yeast cells expressing *MFS11* did not show any alteration of susceptibility (figure 3.10 and figure 3.11). The expression of each plant gene also had no effect on yeast susceptibility or tolerance to  $\text{Na}^+$  (data not shown)



**Figure 3.10 - Effect of the expression of *MFS10* in yeast cells exposed to  $\text{Co}^{2+}$  (1.5 mM),  $\text{Cu}^{2+}$  (0.7 mM) and  $\text{Mn}^{2+}$  (35 mM). Cell suspensions used to prepare the spots were 1:5 (b) and 1:10 (c) dilutions of the cell suspension used in a. These pictures are representative of the results obtained in 3 replicates.**



**Figure 3.11 – Effect of the expression of *MFS11* and *MFS12* in yeast cells exposed to  $\text{Mn}^{2+}$  (35 mM) and  $\text{Cu}^{2+}$  (0.8mM). Cell suspensions used to prepare the spots were 1:5 (b) and 1:10 (c) dilutions of the cell suspension used in a. These pictures are representative of the results obtained in 3 replicates.**

Beside the above mentioned *ZIFL1* expression phenotypes, its expression can also confer susceptibility to yeast cells exposed to cesium (Remy *et al.*, 2013). This finding led us to test the independent expression of the three plant genes in yeast cells exposed to  $\text{Cs}^+$ . The independent expression of each gene conferred increased susceptibility to this cation metal in yeast cells (figure 3.12 and 3.13).

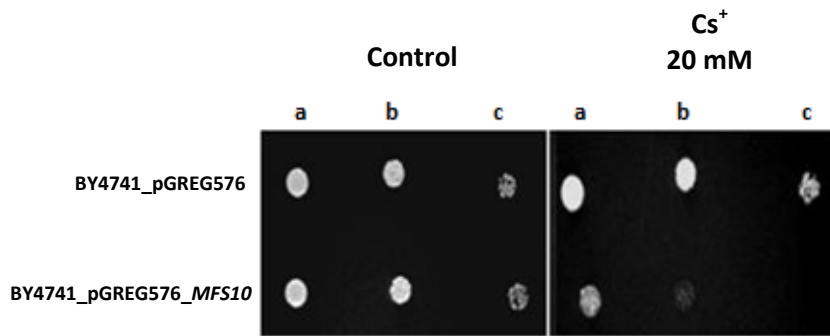


Figure 3.12 – Effect of the expression of *MFS10* in yeast cells exposed to  $\text{Cs}^+$  (20 mM). Cell suspensions used to prepare the spots were 1:5 (b) and 1:10 (c) dilutions of the cell suspension used in a. These pictures are representative of the results obtained in 3 replicates.

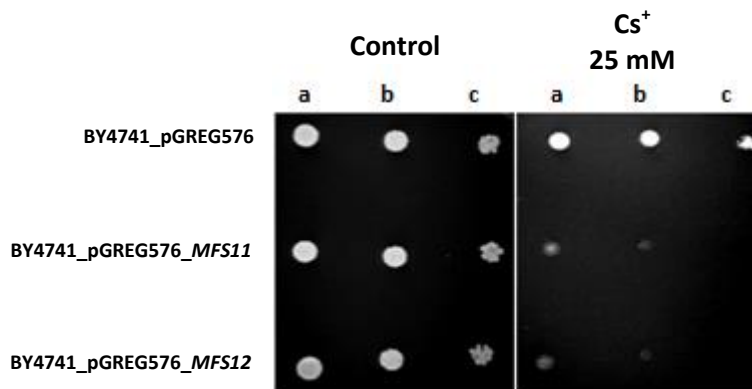
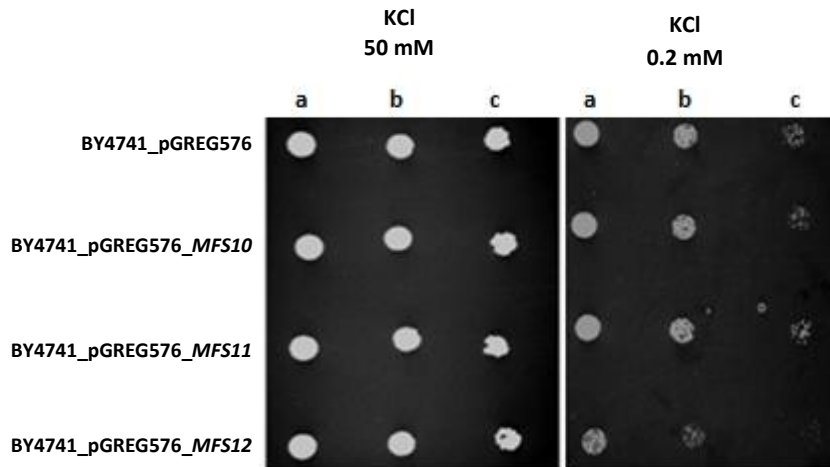


Figure 3.13 – Effect of the expression of *MFS11* and *MFS12* in yeast cells exposed to  $\text{Cs}^+$  (25 mM). Cell suspensions used to prepare the spots were 1:5 (b) and 1:10 (c) dilutions of the cell suspension used in a. These pictures are representative of the results obtained in 3 replicates.

Cesium is an alkali metal with chemical properties similar to potassium ( $\text{K}^+$ ). This cytotoxic metal can perturb plant cellular biochemistry by competing with cellular influx of potassium (White and Broadley, 2000). Therefore, it was investigate whether the *MFS10*, *MFS11* and *MFS12* transporters can influence  $\text{K}^+$  uptake by the yeast cell by evaluating the growth of yeast cells expressing *MFS10*, *MFS11* or *MFS12* genes under limiting potassium concentrations. *MFS10* and *MFS11* apparently did not influence yeast  $\text{K}^+$  uptake, while yeast cells expressing *MFS12* showed increased inhibition under potassium deprivation (figure 3.14).



**Figure 3.14 – Susceptibility to low potassium growth conditions of yeast cells harboring the cloning vector pGREG576 or the plasmids pGREG576\_MFS10, pGREG576\_MFS11 or pGREG576\_MFS12.** Cell suspensions used to prepare the spots were 1:5 (b) and 1:10 (c) dilutions of the cell suspension used in a. These pictures are representative of the results obtained in 3 replicates.

As referred above, the subcellular localization of MFS10 and MFS11 GFP fusion proteins from yeast cells harboring pGREG576 plasmid constructions was not confirmed. Therefore, pGREG596 constructions aimed to optimize the heterologous expression in order to achieve plasma membrane localization. Thus, yeast cells harboring the empty cloning vector pGREG596 or the plasmids pGREG596\_MFS10, and pGREG596\_MFS11 were also examined in the same basal medium supplemented with different compounds.

When exposed to Cs<sup>+</sup>, the growth of yeast cells harboring plasmid pGREG596\_MFS10 or pGREG596\_MFS11 was below the growth of control yeast cells harboring the empty vector (figure 3.15). These results reinforce results from previous spot growth assays with yeast cells harboring pGREG576 plasmid constructions. Given this, yeast cells harboring plasmid pGREG596\_MFS10 or pGREG596\_MFS11 were also tested under potassium deprivation. However, expression of MFS10 and MFS11 from yeast cells harboring the pGREG596 constructions also appear not to influence K<sup>+</sup> uptake (data not shown).

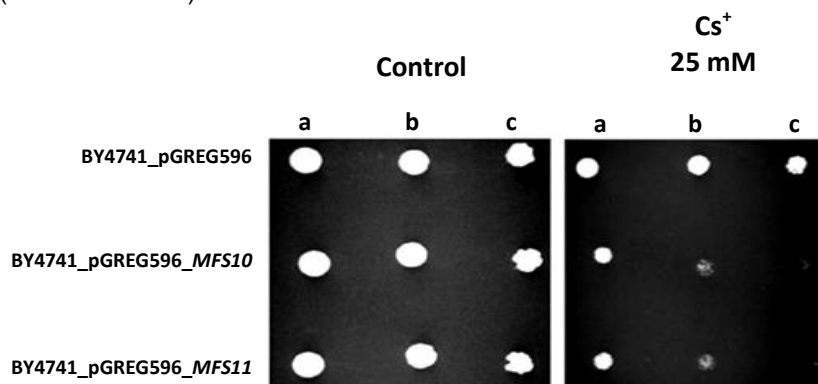


**Figure 3.15 – Effect of the expression of MFS10 and MFS11 in yeast cells exposed to Cs<sup>+</sup> (25 mM).** Cell suspensions used to prepare the spots were 1:5 (b) and 1:10 (c) dilutions of the cell suspension used in a. These pictures are representative of the results obtained in 3 replicates.

All plasmid constructions were also used to transform yeast cells of  $\Delta qdr2$  mutant with the QDR2 gene deleted with aim to assess the ability of the plant transporters to complement the lack of the encoded MFS transporter. This transporter is able to mediate  $K^+$  uptake (Vargas *et al.*, 2004). However, all the yeast cells expressing the different plasmids showed a pattern growth similar to yeast cells harboring the empty vector when exposed to potassium deprivation, including yeast cells expressing the *MFS12* (figure 3.16). All the  $K^+$  deprivation assays appears to suggest that the plant transporters under study did not influence  $K^+$  uptake.

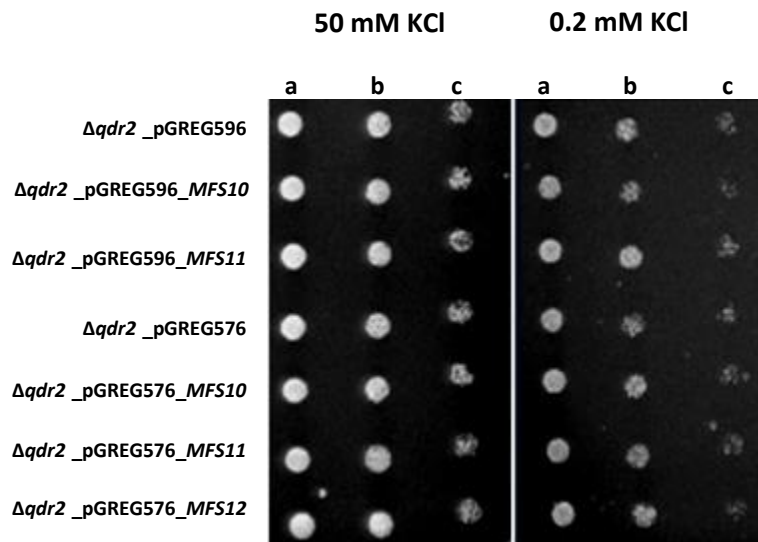


**Figure 3.16 – Susceptibility to low potassium growth conditions of yeast cells harboring the cloning vector pGREG576 or pGREG596 and corresponding derived recombinant plasmids. Cell suspensions used to prepare the spots were 1:5 (b) and 1:10 (c) dilutions of the cell suspension used in a.**

The synthetic auxin 2,4-D is one of the most widely used herbicides and the mechanisms underlying toxicity plant resistance have been mostly described in *S. cerevisiae* (Teixeira *et al.*, 2007). A previous study of *ZIFL1* showed that both isoforms when expressed in yeast cells confer increased resistance to 2,4-D and IAA, which are toxic at high concentrations (Cabrito *et al.*, 2009; Remy *et al.*, 2013). However, the expression of *MFS10*, *MFS11* or *MFS12* genes apparently did not affect yeast susceptibility to these compounds, nor to the other auxin like-herbicide tested MCPA or to the product of 2,4-D degradation, 2,4-DCP (data not show). The herbicide alachlor and metolachlor were also tested. The *ScTPO1* gene expression, a *ZIFL1* homolog, was found to confer resistance to alachlor. Yet, the yeast cells expressing the plant genes under study do not show increased resistance to alachlor or metolachlor (data not shown).

Weak acids are organic acids with physiological impact in plants, as normal metabolites. Acetic acid is also a weak acid able to impose stress to several organisms. Its presence in soil results mainly from anaerobic activity and can lead to plant stress. A few MFS transporters are able to confer resistance to this weak acid, such as the *S. cerevisiae* Azr1p transporter and the *A. thaliana* *ZIFL1* (Tenreiro *et al.*, 2000; Remy *et al.*, 2013). These findings led us to test the influence of weak acids such as malic acid, citric acid and succinic acid in yeast cells expressing the plant genes under study. Apparently, they

did not affect yeast susceptibility to malic acid, citric acid or succinic acid (data not shown). However, the independent expression of each plant gene conferred increased yeast resistance to acetic acid (figure 3.17). Although, yeast cells expressing pGREG576\_ *MFS10* showed increased tolerance to acetic acid, this phenotype was weaker when compared with yeast cells expressing *MFS11* and *MFS12*.

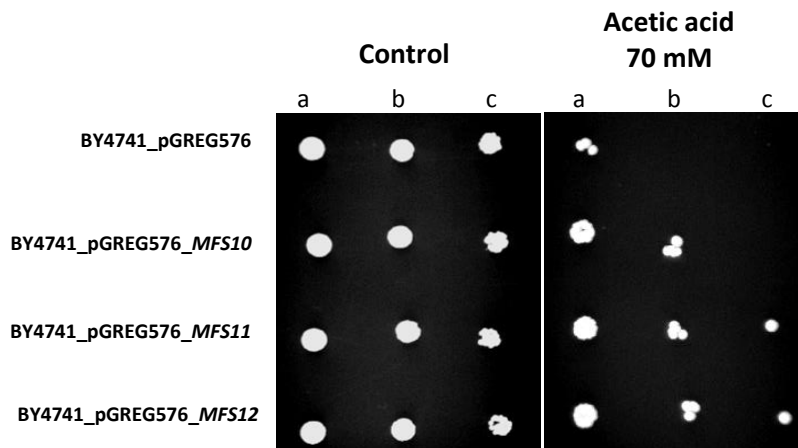


**Figure 3.17 – Effect of the expression of *MFS10*, *MFS11* and *MFS12* in yeast cells exposed to acetic acid (70 mM).** Cell suspensions used to prepare the spots were 1:5 (b) and 1:10 (c) dilutions of the cell suspension used in a. These pictures are representative of the results obtained in 3 replicates.

Yeast cells harboring plasmid pGREG596\_ *MFS10* or pGREG596\_ *MFS11* also showed increased resistance to the presence of acetic acid, when compared to yeast cells harboring the empty cloning vector (figure 3.18 and 3.19). These results are consistent with the result from the acetic acid stress susceptibility assays obtained with yeast cells harboring plasmid pGREG576\_ *MFS10* or pGREG576\_ *MFS11*.

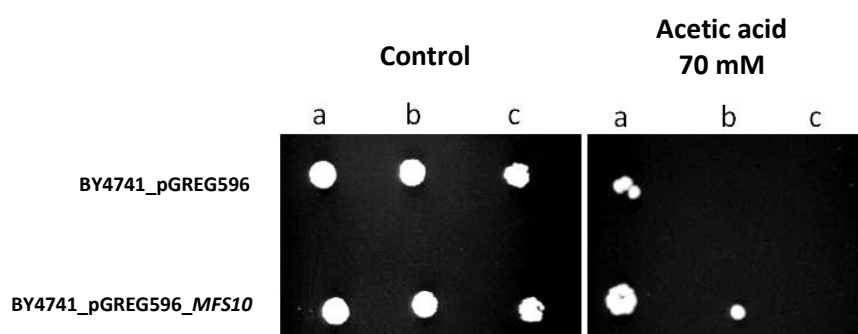


**Figure 3.18 – Effect of the expression of *MFS10* in yeast cells exposed to acetic acid (70 mM).** Cell suspensions used to prepare the spots were 1:5 (b) and 1:10 (c) dilutions of the cell suspension used in a. These pictures are representative of the results obtained in 3 replicates.

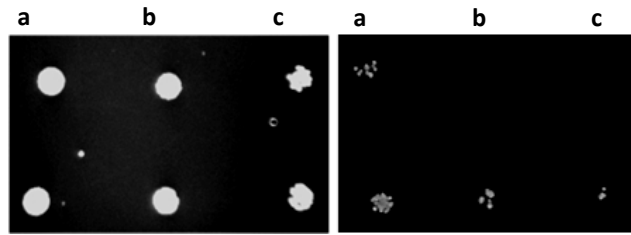


**Figure 3.19 – Effect of the expression of *MFS11* in yeast cells exposed to acetic acid (70 mM). Cell suspensions used to prepare the spots were 1:5 (b) and 1:10 (c) dilutions of the cell suspension used in a. These pictures are representative of the results obtained in 3 replicates.**

Experiments carried out by our IGC partners suggested that *MFS10* expression is involved in response to hyperosmotic in *A. thaliana* under hyperosmotic stress, through the presence of mannitol. This result led us to test the influence of mannitol (1.85 M) in yeast cells expressing the *MFS10*, but, the expression of *MFS10* had no effect on yeast susceptibility to mannitol (figure 3.20).

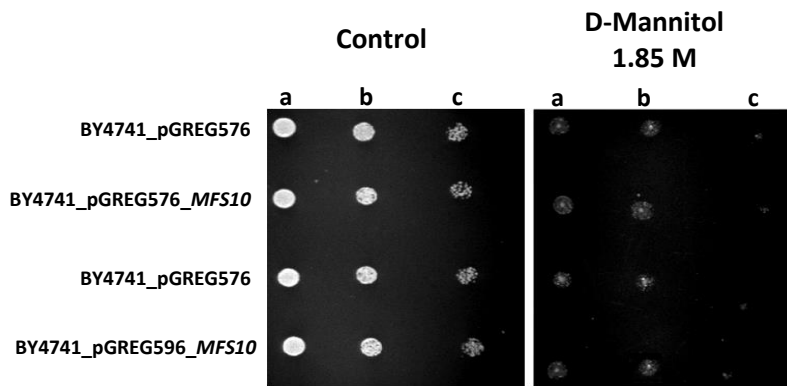


**Figure 3.20 – Effect of the expression of *MFS10* in yeast cells exposed to D-mannitol (1.85 M). Cell suspensions used to prepare the spots were 1:5 (b) and 1:10 (c) dilutions of the cell suspension used in a. These pictures are representative of the results obtained in 3 replicates.**

The expression of *MFS10* or *MFS11*, from yeast cells harboring plasmid pGREG596\_*MFS10* or pGREG596\_*MFS11*, apparently did not result either in increased yeast resistance or susceptibility to  $Al^{3+}$ ,  $Co^{2+}$ ,  $Cu^{2+}$  and  $Mn^{2+}$  and to the other tested compounds (data not shown). The next table is a summary of the results from the growth spots susceptibility assays.

**Table 3.2 – Results from chemical susceptibility spots assays. “R” or “R+” represents yeast cells that exhibited increased tolerance to certain stress due to the expression of a plant gene compared with control cells harboring the cloning vector or compared with yeast cells harboring a plasmid construction, respectively. “S” or “-” represents yeast cells that exhibited decreased or unaltered tolerance due to the expression of a plant gene.**

		BY4741 cells harboring				
		pGREG576_ <i>MFS10</i>	pGREG576_ <i>MFS11</i>	pGREG576_ <i>MFS12</i>	pGREG596_ <i>MFS10</i>	pGREG596_ <i>MFS11</i>
Tested compounds*	Acetic acid	R	R <sup>+</sup>	R <sup>+</sup>	R	R <sup>+</sup>
	Cs <sup>+</sup>	S	S	S	S	S
	Al <sup>3+</sup>	S	-	-	-	-
	Co <sup>2+</sup>	S	-	-	-	-
	Cu <sup>2+</sup>	S	-	S	-	-
	Mn <sup>2+</sup>	R	R	R	-	-
	K <sup>+</sup> deprivation	-	-	S	-	-

\*Apparently the expression of any of the plant transporters was not able to confer increased or decreased tolerance to the others tested compounds namely: Cd<sup>2+</sup>, Fe<sup>3+</sup>, Ni<sup>+</sup>, TI<sup>3+</sup>, Zn<sup>2+</sup>, 2,4-D, MCPA, 2,4-DCP, IAA, L-Malic Acid, Citric Acid, Succinic acid, Alachlor, metolachlor and D-mannitol.

## 4. Discussion

The expression in yeast cells of the plant genes *MFS10*, *MFS11* and *MFS12*, presumably encoding transporters of the MFS, was carried out envisaging their sub-cellular localization and the assessment of the susceptibility to chemical stresses of yeast cells expressing the referred plant genes.

Based on PSORT prediction (<http://psort.hgc.jp/form.html>) the *A. thaliana* proteins MFS10 and MFS11 have a plasma membrane localization, while MFS12 is most probably located at the endoplasmic reticulum membrane.

Consistent with these predictions, *A. thaliana* protoplast localization assays, performed by our IGC collaborators, showed a plasma membrane localization for GFP-MFS10 and GFP-MFS11 fusion proteins (figure 4.1). Given this, it is likely that, when expressed in yeast, these transporters may also localize at the plasma membrane.

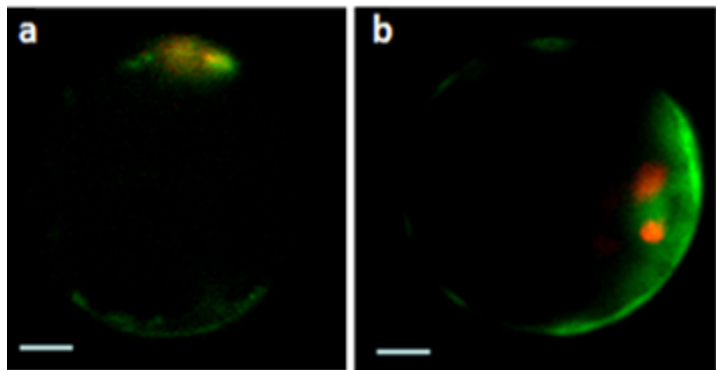


**Figure 4.1 - Confocal laser scanning microscopy images of *A. thaliana* wild-type mesophyll protoplasts transiently expressing either MFS10-GFP (a) or MFS11-GFP (b). Bars = 20  $\mu$ m (results supplied by our IGC collaborators).**

The cloning vector pGREG576 was

successfully used in our laboratory to localize other plant proteins (Remy *et al.*, 2012), even those with a non-plasma membrane localization in plant, at the yeast plasma membrane (Remy *et al.*, 2013). However, the expression of *MFS10* and *MFS11* genes when inserted in pGREG576 showed that the GFP-fused-proteins accumulated in the yeast cytosol as fluorescent dots. Although no detectable fluorescence could be observed at plasma membrane, the possibility that these plant transporters localized at plasma membrane as well cannot be excluded and, based on the consistent susceptibility/resistance phenotypes registered, this is a likely possibility.

New plasmid constructions were carried out, this time using the cloning vector pGREG596 to insert *MFS10* and *MFS11*, in order to force plant transporters to localize at yeast plasma membrane. When expressed in yeast from these recombinant plasmids, GFP-MFS10 and GFP-MFS11 fusion proteins were observed as fluorescence spots at specific regions of plasma membrane. Since fluorescence was not uniformly distributed in plasma membrane, the full functionality of these proteins is in doubt.

Overexpression of heterologous transmembrane proteins may be toxic for the hosting cell physiology, as reported before for other plant transporters, where these toxic effects were associated to the loss of a full functional activity and to an improper plasma membrane localization of the plant transporter when expressed in yeast (Haro *et al.*, 2005; Ito & Gray, 2006). Indeed, the accumulation of fluorescent dots in the cytosol over time was observed in yeast cells expressing *MFS10*, *MFS11* and *MFS12* genes. Such accumulation of improperly localized GFP-fused-protein resulting from their

overexpression can also mask the fluorescence associated to the protein that could have been properly localized at plasma membrane.

The different galactose concentrations tested to induce protein expression from the plasmid constructions and the swap of the cloning vector aimed at optimizing the functional protein expression in yeast. It can be speculated that these plant sequences could not be properly recognized by the yeast machinery, resulting in their mislocalization or in protein misfolding. In other studies, the plant full-length Pht4;1 or Pht2;1 transporters were sequestered in an internal compartment when expressed in yeast. Only truncated versions of these transporters were able to localize at the yeast plasma membrane (Versaw & Harrison, 2002; Guo *et al.*, 2008). However, their truncated version appears to rely on a deletion of the transit peptide associated to a natural internal localization in *A. thaliana*. This issue was not considered when this work was planned and we can only raise this hypothesis at this time.

Nevertheless, it is important to highlight that yeast chemical stress susceptibility results suggest a functional activity for these transporters when expressed in yeast independently of the cloning vector used, which is consistent with a plasma membrane localization or at least with a functional membrane localization.

Concerning the MFS12-GFP fusion protein, it was possible to observe a plasma membrane and an internal membrane localization, presumably at the endoplasmic reticulum membrane. The endoplasmic reticulum is a single continuous membrane-enclosed organelle with distinct functions and closely associated with other cell organelle membranes, such as the plasma membrane (Staehelein *et al.*, 1997; Englis *et al.*, 2009). Endoplasmic reticulum membrane localization of MFS12-fused-protein is in agreement with the above referred PSORT prediction and with plant assays, since MFS12-GFP appears to have an internal localization in plant protoplasts (figure 4.2). Curiously, MFS12 was suggested to be involved in oligopeptide transport (<https://www.genevestigator.com>). The yeast transporter Aqr1p despite an internal vesicle and plasma membrane localization, it is involved in amino acids export and it has been implicated in yeast tolerance to weak acids (Velasco *et al.*, 2004). These similarities between MFS12 and Aqr1p are worthwhile to be considered in future studies on the MFS12 biological role.

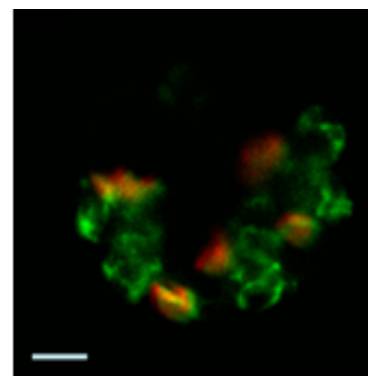


**Figure 4.2 - Confocal laser scanning microscopy images of *A. thaliana* wild-type mesophyll protoplasts transiently expressing MFS12-GFP. Bars = 20 mm (results supplied by our IGC collaborators).**

One of the main advantages of employing the heterologous expression yeast system is the possibility to perform a large screening of potential substrate in a relatively easy and short way and to carry out transport assays for selected substrates. Given this, and guided by a few indications coming from microarray data in the literature and results from ZIFL1 experiments, chemical stress susceptibility assays with several compounds of agricultural relevance were performed.

The three plant genes under study were found to confer susceptibility to  $\text{Cs}^+$  in yeast. These results were observed for yeast cells expressing each gene from the two different plasmid constructions prepared. The non-essential cation  $\text{Cs}^+$  is assimilated by all organisms and at millimolar concentrations is toxic.  $\text{Cs}^+$  has chemical properties similar to  $\text{K}^+$ . Therefore,  $\text{Cs}^+$  can compete with  $\text{K}^+$  for uptake into the cell, leading to  $\text{K}^+$  starvation (Avery, 1995; White & Broadley, 2000). Given this, MFS10, MFS11 and MFS12 transporters were hypothesized to have  $\text{K}^+$  uptake capacity, which will be reflected in an increased yeast tolerance to  $\text{K}^+$  deprivation. However, their expression in parental or  $\Delta qdr2$  mutant strains under  $\text{K}^+$  deprivation appeared not to lead to increased  $\text{K}^+$  uptake. It is possible that these transporters have a low affinity for  $\text{K}^+$ , which consequently renders difficult the assessment of the eventual increase of  $\text{K}^+$  uptake. For example, the secondary transporter AtKT2, when expressed in yeast  $\Delta trk1\Delta trk2$  mutant strain was able to complement the yeast growth at a  $\text{K}^+$  concentration of 2.5 mM, while at lower concentrations this capacity was lost (Quintero & Blatt, 1997). The expression of MFS12 in yeast parental strain was found to lead to an increased susceptibility to  $\text{K}^+$  deprivation. The mislocalization of this transporter or even a toxic effect of its heterologous expression in the yeast cell might have led to this phenotype.

The three plant transporters were able to confer yeast resistance to acetic acid. Once in the cytosol, the weak acid dissociates releasing protons and the respective counterion. The ZIFL1 transporter was also found to confer increased tolerance to acetic acid when expressed in yeast (Remy *et al.*, 2013). Given this, it is reasonable to hypothesize that the plant transporters MFS10, MFS11 and MFS12 may be involved in cell protection against the acetic acid. Although this increased resistance may happen through the extrusion of acetate to the extracellular medium, it is possible that this increased tolerance occurs fortuitously or opportunistically, as reported before for other MFS transporters (Fernandes *et al.*, 2005). The demonstration of a direct efflux will require the performance of transport assays.

The expression of MFS10 and MFS11 in yeast cells harboring pGREG576 constructions conferred increased resistance to  $\text{Mn}^{2+}$ , an essential trace element that can be accumulated and utilized by several organisms (Cobbett, 2000). Additionally, the expression of MFS10 inserted in plasmid pGREG576\_MFS10 confers increased susceptibility to high concentrations of  $\text{Al}^{3+}$ ,  $\text{Co}^{2+}$  and  $\text{Cu}^{2+}$  in yeast. However, the expression of these genes in yeast cells harboring pGREG596 constructions did not lead to these metal phenotypes. If the plant gene functional expression from pGREG596 was below the levels from the other plasmid, an increased expression of these genes through the pGREG596 could lead to similar phenotypes. On other hand, the above referred likely mislocalization in yeast cells expressing pGREG576 construction could explain these phenotypes, due to an increased transport of these metals across internal membranes either than across plasma membrane.

Alternatively, and concerning yeast cells harboring pGREG576\_MFS10, the heterologous expression can affect yeast physiology and even viability, which can lead to an increased susceptibility to toxic concentrations of the referred tested compounds. Moreover, although MFS10 expression conferred increased resistance to acetic acid, the level of increased resistance was below the one conferred by MFS11 and MFS12 expression. Incorrect heterologous expression of MFS10, such as, partial plasma membrane localization, mislocalization or misfolding, can eventually be reflected in a weaker

phenotype, like a more subtle resistance to acetic acid. Also, in yeast cells harboring pGREG576 constructions, MFS11-GFP fusion protein are present in the cell periphery, while MFS10-GFP fusion protein observation showed fluorescent dots throughout the cell.

Yeast cells harboring plasmid pGREG576\_ *MFS12* showed increased susceptibility to  $\text{Cu}^{2+}$  and increased resistance to  $\text{Mn}^{2+}$  but there is no evidence to support the proposal that MFS12 mediates  $\text{Cu}^{2+}$  and  $\text{Mn}^{2+}$  transport across plasma membrane or across an internal membrane. The successful cloning of *MFS12* into pGREG596 and a correct sub-cellular heterologous localization of *MFS12* expression in yeast may help to clarify the place and direction of these metals transport in the cell.

Gene expression analysis of *A. thaliana* revealed that *MFS10* gene is upregulated when subjected to mannitol or salt. Moreover, the *A. thaliana mfs10* null mutant is insensitive to salt and hyperosmotic stress at germination (figure 3.20). Mannitol appears to influence osmotic stress tolerance by serving as a compatible solute or osmoprotectant (Bohnert & Jensen, 1996). Given this, it is likely that MFS10 transporter may be somehow related to osmotic stress tolerance in plant.

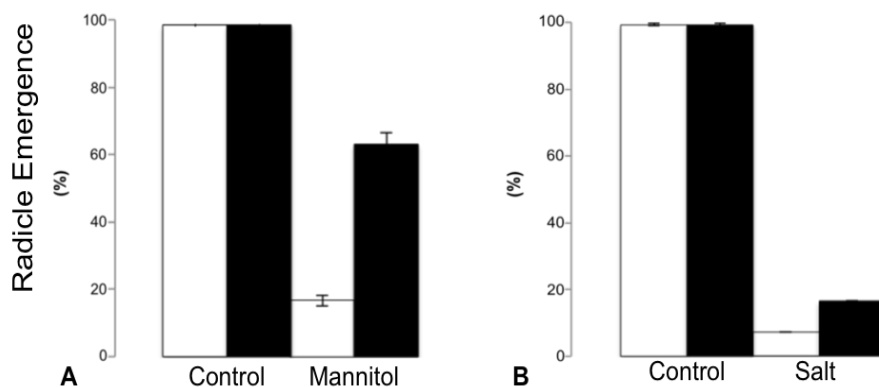


**Figure 3.21 - Osmotic and salt phenotypes of the *mfs10* mutant. Germination (radicle emergence) rates of *A. thaliana* Col-0 (open bars) and *mfs10* null mutant (closed bars) seedlings grown in control conditions or in the presence of 400mM mannitol (A) or 250 mM salt (B) (means  $\pm$  SE, n=3) (supplied by our IGC collaborators).**

However, yeast cells harboring pGREG576\_ *MFS10* or pGREG596\_ *MFS10* did not show any increase in the resistance to salt or mannitol. No explanation for this different behaviour of MFS10 in yeast and in plant can be given at this time, except that the transporter could have been mislocalized in yeast.

The plant transporters when expressed in yeast cells can mediate substrate transport across plasma membrane or across internal membranes. The above referred cytotoxic compounds, such as  $\text{Cs}^{2+}$  or acetate can be directly or indirectly transported across cell membranes by the action of these transporters. The altered partitioning model suggests that transporters may have an indirect action, and do not transport all the substrates to which they confer increase tolerance by themselves, but through an alteration of intracellular pH and/or plasma membrane potential related with their biological function in the transport of physiologic substrates (Roepe *et al.*, 1996). Moreover, since no transport activity assays were performed in this study it is impossible to go further in the conclusions.

As a whole, the results gathered for these three transporters, in *S. cerevisiae* and *A. thaliana* suggest several possible substrates for these transporters. However, it is not possible at this time to anticipate the main substrate for these transporters. The acetic acid and Cs<sup>2+</sup> phenotypes registered in yeast may occur fortuitously and at this time these potential substrates cannot be proposed without any transport accumulation assays. The study of MFS10, MFS11 and MFS12 is still in a preliminary phase, but the unicellular *S. cerevisiae* has provided a number of indications of interest to proceed with this work in plant and in yeast.

## 5. References

- Abramson J, Smirnova I, Kasho V, Verner G, Kaback HR, Iwata S. 2003.** Structure and mechanism of the lactose permease of *Escherichia coli*. *Science (New York, N.Y.)* **301**: 610–5.
- Antebi A, Fink GR. 1992.** The yeast Ca<sup>2+</sup>-ATPase homologue, PMR1, is required for normal Golgi function and localizes in a novel Golgi-like distribution. *Molecular biology of the cell* **3**: 633–54.
- Araújo WL, Fernie AR, Nunes-Nesi A. 2011.** Control of stomatal aperture: a renaissance of the old guard. *Plant signaling & behavior* **6**: 1305–11.
- Avery S V. 1995.** Caesium accumulation by microorganisms: uptake mechanisms, cation competition, compartmentalization and toxicity. *Journal of Industrial Microbiology* **14**: 76–84.
- Bennett MJ, Marchant A, Green HG, May ST, Ward SP, Millner PA, Walker AR, Schulz B, Feldmann KA. 1996.** Arabidopsis AUX1 Gene: a permease-like regulator of root gravitropism. *Science (New York, N.Y.)* **273**: 948–50.
- Bialeski RL. 1973.** Phosphate pools, phosphate transport, and phosphate availability. *Annual Review of Plant Physiology and Plant Molecular Biology* **24**: 225–252.
- Blakeslee JJ, Bandyopadhyay A, Lee OR, Mravec J, Titapiwatanakun B, Sauer M, Makam SN, Cheng Y, Bouchard R, Adamec J, et al. 2007.** Interactions among PIN-FORMED and P-glycoprotein auxin transporters in Arabidopsis. *The Plant Cell* **19**: 131–47.
- Bohnert HJ, Jensen RG. 1996.** Strategies for engineering water-stress tolerance in plants. *Trends in Biotechnology* **14**: 89–97.
- Brockmann K. 2009.** The expanding phenotype of GLUT1-deficiency syndrome. *Brain & development* **31**: 545–52.
- Bun-Ya M, Nishimura M, Harashima S, Oshima Y. 1991.** The PHO84 Gene of *Saccharomyces cerevisiae* encodes an inorganic phosphate transporter. *Molecular and Cellular Biology* **11**: 3229–38.
- Büttner M. 2007.** The monosaccharide transporter(-like) Gene family in Arabidopsis. *FEBS letters* **581**: 2318–24.
- Cabrilo TR, Teixeira MC, Duarte A a, Duque P, Sá-Correia I. 2009.** Heterologous expression of a Tpo1 homolog from Arabidopsis thaliana confers resistance to the herbicide 2,4-D and other chemical stresses in yeast. *Applied Microbiology and biotechnology* **84**: 927–36.

- Cerezo M, Tillard P, Filleur S, Muños S, Daniel-Vedele F, Gojon A. 2001.** Major alterations of the regulation of root NO<sub>3</sub><sup>-</sup> uptake are associated with the mutation of Nrt2.1 and Nrt2.2 Genes in Arabidopsis. *Plant Physiology* **127**: 262–71.
- Cherry JM, Hong EL, Amundsen C, Balakrishnan R, Binkley G, Chan ET, Christie KR, Costanzo MC, Dwight SS, Engel SR, et al. 2012.** Saccharomyces Genome Database: the genomics resource of budding yeast. *Nucleic Acids Research* **40**: D700–5.
- Cobbett CS. 2000.** Phytochelatin and their roles in heavy metal detoxification. *Plant Physiology* **123**: 825–32.
- Cubero B, Nakagawa Y, Jiang X-Y, Miura K-J, Li F, Raghothama KG, Bressan RA, Hasegawa PM, Pardo JM. 2009.** The phosphate transporter PHT4;6 is a determinant of salt tolerance that is localized to the Golgi apparatus of Arabidopsis. *Molecular Plant* **2**: 535–52.
- Daram P, Brunner S, Persson BL, Amrhein N, Bucher M. 1998.** Functional analysis and cell-specific expression of a phosphate transporter from tomato. *Planta* **206**: 225–33.
- Desai PN, Shrivastava N, Padh H. 2010.** Production of heterologous proteins in plants: strategies for optimal expression. *Biotechnology advances* **28**: 427–35.
- Dos Santos SC, Teixeira MC, Cabrito TR, Sá-Correia I. 2012.** Yeast toxicogenomics: genome-wide responses to chemical stresses with impact in environmental health, pharmacology, and biotechnology. *Plant Cell* **3**: 63.
- Emanuelsson O, Nielsen H, Brunak S, von Heijne G. 2000.** Predicting subcellular localization of proteins based on their N-terminal amino acid sequence. *Journal of molecular biology* **300**: 1005–16.
- English AR, Zurek N, Voeltz GK. 2009.** Peripheral ER structure and function. *Current opinion in cell biology* **21**: 596–602.
- Felder T, Bogengruber E, Tenreiro S, Ellinger A, Sá-Correia I, Briza P. 2002.** Dtr1p, a multidrug resistance transporter of the major facilitator superfamily, plays an essential role in spore wall maturation in *Saccharomyces cerevisiae*. *Eukaryotic Cell* **1**: 799–810.
- Fernandes AR, Mira NP, Vargas RC, Canelhas I, Sá-Correia I. 2005.** *Saccharomyces cerevisiae* adaptation to weak acids involves the transcription factor Haa1p and Haa1p-regulated Genes. *Biochemical and Biophysical Research Communications* **337**: 95–103.
- Ferro M, Salvi D, Brugière S, Miras S, Kowalski S, Louwagie M, Garin J, Joyard J, Rolland N. 2003.** Proteomics of the chloroplast envelope membranes from *Arabidopsis thaliana*. *Molecular & cellular proteomics* : *MCP* **2**: 325–45.

**Frommer WB, Ninnemann O. 1995.** Heterologous expression of Genes in bacteria, fungal, animal, and plant cells. *Annual Review of Plant Physiology and Plant Molecular Biology* **46**: 419–444.

**Geisler M, Blakeslee JJ, Bouchard R, Lee OR, Vincenzetti V, Bandyopadhyay A, Titapiwatanakun B, Peer WA, Bailly A, Richards EL, et al. 2005.** Cellular efflux of auxin catalyzed by the Arabidopsis MDR/PGP transporter AtPGP1. *The Plant Journal : for Cell and Molecular Biology* **44**: 179–94.

**Goffeau A, Barrell BG, Bussey H, Davis RW, Dujon B, Feldmann H, Galibert F, Hoheisel JD, Jacq C, Johnston M, et al. 1996.** Life with 6000 Genes. *Science (New York, N.Y.)* **274**: 546, 563–7.

**Goswitz VC, Brooker RJ. 1995.** Structural features of the uniporter/symporter/antiporter superfamily. *Protein science : a publication of the Protein Society* **4**: 534–7.

**Guo B, Jin Y, Wussler C, Blancaflor EB, Motes CM, Versaw WK. 2008.** Functional analysis of the Arabidopsis PHT4 family of intracellular phosphate transporters. *The New phytologist* **177**: 889–98.

**Hampton CR, Bowen HC, Broadley MR, Hammond JP, Mead A, Payne KA, Pritchard J, White PJ, Hri W, Cv W, et al. 2004.** Cesium Toxicity in Arabidopsis 1. **136**: 3824–3837.

**Haro R, Bañuelos M, Senn EM, Barrero-gil J, Rodríguez-Navarro A. 2005.** HKT1 Mediates Sodium Uniport in Roots . Pitfalls in the Expression of HKT1 in Yeast 1. *Plant Physiology* **139**: 1495–1506.

**Haydon MJ, Cobbett CS. 2007.** A novel major facilitator superfamily protein at the tonoplast influences zinc tolerance and accumulation in Arabidopsis. *Plant Physiology* **143**: 1705–19.

**Henderson PJF, Baldwin S a. 2013.** This is about the in and the out. *Nature Structural & Molecular Biology* **20**: 654–5.

**Henderson PJ, Maiden MC. 1990.** Homologous sugar transport proteins in Escherichia coli and their relatives in both prokaryotes and eukaryotes. *Philosophical transactions of the Royal Society of London. Series B, Biological Sciences* **326**: 391–410.

**Higgins CF. 1992.** ABC transporters: from microorganisms to man. *Annual Review of cell Biology* **8**: 67–113.

**Higgins CF. 2007.** Multiple molecular mechanisms for multidrug resistance transporters. *Nature* **446**: 749–57.

**Hillenmeyer ME, Fung E, Wildenhain J, Pierce SE, Hoon S, Lee W, Proctor M, St Onge RP, Tyers M, Koller D, et al. 2008.** The chemical genomic portrait of yeast: uncovering a phenotype for all Genes. *Science (New York, N.Y.)* **320**: 362–5.

- Hohmann S, Mager WH (Eds.). 2003.** *Yeast Stress Responses*. Berlin, Heidelberg: Springer Berlin Heidelberg.
- Ito H, Gray WM. 2006.** A gain-of-function mutation in the Arabidopsis pleiotropic drug resistance transporter PDR9 confers resistance to auxinic herbicides. *Plant Physiology* **142**: 63–74.
- Jansen G, Wu C, Schade B, Thomas DY, Whiteway M. 2005.** Drag&Drop cloning in yeast. *Gene* **344**: 43–51.
- Jungwirth H, Kuchler K. 2006.** Yeast ABC transporters-- a tale of sex, stress, drugs and aging. *FEBS letters* **580**: 1131–8.
- Kanazawa S, Driscoll M, Struhl K. 1988.** ATR1, a *Saccharomyces cerevisiae* Gene encoding a transmembrane protein required for aminotriazole resistance. *Molecular and Cellular Biology* **8**: 664–73.
- Kartner N, Ling V. 1983.** Cell surface P-glycoprotein associated with multidrug resistance in mammalian cell lines. *Science* **221**: 1285–1288.
- Kiba T, Feria-Bourrellier A-B, Lafouge F, Lezhneva L, Boutet-Mercey S, Orsel M, Bréhaut V, Miller A, Daniel-Vedele F, Sakakibara H, et al. 2012.** The Arabidopsis nitrate transporter NRT2.4 plays a double role in roots and shoots of nitrogen-starved plants. *The Plant Cell* **24**: 245–58.
- Kulkarni MM, Booker M, Silver SJ, Friedman A, Hong P, Perrimon N, Mathey-Prevoit B. 2006.** Evidence of off-target effects associated with long dsRNAs in *Drosophila melanogaster* cell-based assays. *Nature Methods* **3**: 833–8.
- Law CJ, Maloney PC, Wang D. 2008.** Ins and Outs of Major Facilitator Superfamily Antiporters. *Annual review of Microbiology*: 289–305.
- Leggewie G, Willmitzer L, Riesmeier JW. 1997.** Two cDNAs from potato are able to complement a phosphate uptake-deficient yeast mutant: identification of phosphate transporters from higher plants. *The Plant Cell* **9**: 381–92.
- Li F, Ma C, Wang X, Gao C, Zhang J, Wang Y, Cong N, Li X, Wen J, Yi B, et al. 2011.** Characterization of Sucrose transporter alleles and their association with seed yield-related traits in *Brassica napus* L. *BMC Plant Biology* **11**: 168.
- Liu H, Trieu a T, Blaylock L a, Harrison MJ. 1998.** Cloning and characterization of two phosphate transporters from *Medicago truncatula* roots: regulation in response to phosphate and to colonization by arbuscular mycorrhizal (AM) fungi. *Molecular Plant-microbe Interactions : MPMI* **11**: 14–22.

**Marger MD, Saier MH. 1993.** A major superfamily of transmembrane facilitators that catalyse uniport, symport and antiport. *Trends in Biochemical Sciences* **18**: 13–20.

**Mimura T, Dietz K-J, Kaiser W, Schramm MJ, Kaiser G, Heber U. 1990.** Phosphate transport across biomembranes and cytosolic phosphate homeostasis in barley leaves. *Planta* **180**.

**Misson J, Thibaud M-C, Bechtold N, Raghothama K, Nussaume L. 2004.** Transcriptional regulation and functional properties of Arabidopsis Pht1;4, a high affinity transporter contributing greatly to phosphate uptake in phosphate deprived plants. *Plant Molecular Biology* **55**: 727–41.

**Mitchell P. 1967.** Translocations through natural membranes. *Advances in enzymology and related areas of molecular biology* **29**: 33–87.

**Mitsukawa N, Okumura S, Shirano Y, Sato S, Kato T, Harashima S, Shibata D. 1997.** Overexpression of an Arabidopsis thaliana high-affinity phosphate transporter Gene in tobacco cultured cells enhances cell growth under phosphate-limited conditions. *Proceedings of the National Academy of Sciences of the United States of America* **94**: 7098–102.

**Muchhal US, Pardo JM, Raghothama KG. 1996.** Phosphate transporters from the higher plant Arabidopsis thaliana. *Proceedings of the National Academy of Sciences of the United States of America* **93**: 10519–10523.

**Nagarajan VK, Jain A, Poling MD, Lewis AJ, Raghothama KG, Smith AP. 2011.** Arabidopsis Pht1;5 mobilizes phosphate between source and sink organs and influences the interaction between phosphate homeostasis and ethylene signaling. *Plant Physiology* **156**: 1149–63.

**Nagata T, Iizumi S, Satoh K, Kikuchi S. 2008.** Comparative molecular biological analysis of membrane transport Genes in organisms. *Plant molecular biology* **66**: 565–85.

**Neyfakh AA. 1997.** Natural functions of bacterial multidrug transporters. *Trends in Microbiology* **5**: 309–13.

**Neuhäuser B, Dynowski M, Mayer M, Ludewig U. 2007.** Regulation of NH<sub>4</sub><sup>+</sup> transport by essential cross talk between AMT monomers through the carboxyl tails. *Plant Physiology* **143**: 1651–1659.

**Nunes CIAA, Tenreiro S, Sá-Correia I. 2001.** Resistance and Adaptation to Quinidine in *Saccharomyces cerevisiae*: Role of QDR1 ( YIL120w ), Encoding a Plasma Membrane Transporter of the Major Facilitator Superfamily Required for Multidrug Resistance. *Antimicrobial Agents and Chemotherapy* **45**: 1528–1534.

**Nussaume L, Kanno S, Javot H, Marin E, Pochon N, Ayadi A, Nakanishi TM, Thibaud M-C. 2011.** Phosphate Import in Plants: Focus on the PHT1 Transporters. *Frontiers in Plant Science* **2**: 83.

- Okamoto M, Vidmar JJ, Glass ADM. 2003.** Regulation of NRT1 and NRT2 Gene families of *Arabidopsis thaliana*: responses to nitrate provision. *Plant & Cell Physiology* **44**: 304–17.
- Orsel M, Chopin F, Leleu O, Smith SJ, Krapp A, Daniel-Vedele F, Miller AJ. 2006.** Characterization of a two-component high-affinity nitrate uptake system in *Arabidopsis*. Physiology and protein-protein interaction. *Plant Physiology* **142**: 1304–17.
- Orsel M, Filleur S, Fraisier V, Daniel-Vedele F. 2002.** Nitrate transport in plants: which Gene and which control? *Journal of experimental botany* **53**: 825–33.
- Ozcan S, Johnston M. 1999.** Function and regulation of yeast hexose transporters. *Microbiology and molecular biology reviews : MMBR* **63**: 554–69.
- Pao SS, Paulsen IANT, Saier MH. 1998.** Major Facilitator Superfamily. *Microbiology and Molecular Biology Reviews* **62**: 1–34.
- Paulsen IT, Brown MH, Littlejohn TG, Mitchell BA, Skurray RA. 1996.** Multidrug resistance proteins QacA and QacB from *Staphylococcus aureus*: membrane topology and identification of residues involved in substrate specificity. *Proceedings of the National Academy of Sciences of the United States of America* **93**: 3630–5.
- Petrásek J, Mravec J, Bouchard R, Blakeslee JJ, Abas M, Seifertová D, Wisniewska J, Tadele Z, Kubes M, Covanová M, et al. 2006.** PIN proteins perform a rate-limiting function in cellular auxin efflux. *Science (New York, N.Y.)* **312**: 914–8.
- Peiter E, Montanini B, Gobert A, Pedas P, Husted S, Maathuis FJM, Blaudez D, Chalot M, Sanders D. 2007.** A secretory pathway-localized cation diffusion facilitator confers plant manganese tolerance. *Proceedings of the National Academy of Sciences of the United States of America* **104**: 8532–7.
- Piper P, Mahé Y, Thompson S, Pandjaitan R, Holyoak C, Egner R, Mühlbauer M, Coote P, Kuchler K. 1998.** The pdr12 ABC transporter is required for the development of weak organic acid resistance in yeast. *The EMBO journal* **17**: 4257–65.
- Qi Z, Hampton CR, Shin R, Barkla BJ, White PJ, Schachtman DP. 2008.** The high affinity K<sup>+</sup> transporter AtHAK5 plays a physiological role in planta at very low K<sup>+</sup> concentrations and provides a caesium uptake pathway in *Arabidopsis*. *Journal of Experimental Botany* **59**: 595–607.
- Quintero FJ, Blatt MR. 1997.** A new family of K<sup>+</sup> transporters from *Arabidopsis* that are conserved across phyla. *FEBS Letters* **415**: 206–211.

**Rae AL, Cybinski DH, Jarmey JM, Smith FW. 2003.** Characterization of two phosphate transporters from barley; evidence for diverse function and kinetic properties among members of the Pht1 family. *Plant Molecular Biology* **53**: 27–36.

**Raghothama KG. 1999.** Phosphate Acquisition. *Annual review of plant Physiology and plant molecular biology* **50**: 665–693.

**Reddy VS, Shlykov M a, Castillo R, Sun EI, Saier MH. 2012.** The major facilitator superfamily (MFS) revisited. *The FEBS journal* **279**: 2022–35.

**Reifenberger E, Freidel K, Ciriacy M. 1995.** Identification of novel HXT Genes in *Saccharomyces cerevisiae* reveals the impact of individual hexose transporters on glycolytic flux. *Molecular Microbiology* **16**: 157–67.

**Remy E, Cabrito TR, Baster P, Batista R a, Teixeira MC, Friml J, Sá-Correia I, Duque P. 2013.** A major facilitator superfamily transporter plays a dual role in polar auxin transport and drought stress tolerance in *Arabidopsis*. *The Plant Cell* **25**: 901–26.

**Remy E, Cabrito TR, Batista R a, Teixeira MC, Sá-Correia I, Duque P. 2012.** The Pht1;9 and Pht1;8 transporters mediate inorganic phosphate acquisition by the *Arabidopsis thaliana* root during phosphorus starvation. *The New phytologist* **195**: 356–71.

**Roepe PD, Wei LY, Hoffman MM, Fritz F. 1996.** Altered drug translocation mediated by the MDR protein: direct, indirect, or both? *Journal of Bioenergetics and Biomembranes* **28**: 541–55.

**Roth C, Menzel G, Petétot JM-C, Rochat-Hacker S, Poirier Y. 2004.** Characterization of a protein of the plastid inner envelope having homology to animal inorganic phosphate, chloride and organic-anion transporters. *Planta* **218**: 406–16.

**Sá-Correia I, dos Santos SC, Teixeira MC, Cabrito TR, Mira NP. 2009.** Drug:H<sup>+</sup> antiporters in chemical stress response in yeast. *Trends in Microbiology* **17**: 22–31.

**Sá-Correia I, Tenreiro S. 2002.** The multidrug resistance transporters of the major facilitator superfamily, 6 years after disclosure of *Saccharomyces cerevisiae* genome sequence. *Journal of Biotechnology* **98**: 215–26.

**Scheffer IE. 2012.** GLUT1 deficiency: a glut of epilepsy phenotypes. *Neurology* **78**: 524–5.

**Shimazu M, Sekito T, Akiyama K, Ohsumi Y, Kakinuma Y. 2005.** A family of basic amino acid transporters of the vacuolar membrane from *Saccharomyces cerevisiae*. *The Journal of Biological Chemistry* **280**: 4851–7.

**Shin H, Shin H-S, Dewbre GR, Harrison MJ. 2004.** Phosphate transport in Arabidopsis: Pht1;1 and Pht1;4 play a major role in phosphate acquisition from both low- and high-phosphate environments. *The Plant Journal : for Cell and Molecular Biology* **39**: 629–42.

**Del Sorbo G, Schoonbeek H, De Waard MA. 2000.** Fungal transporters involved in efflux of natural toxic compounds and fungicides. *Fungal Genetics and Biology : FG & B* **30**: 1–15.

**Staelin LA. 1997.** The plant ER: a dynamic organelle composed of a large number of discrete functional domains. *The Plant Journal : for Cell and Molecular Biology* **11**: 1151–65.

**Stratford M, Anslow PA. 1996.** Comparison of the inhibitory action on *Saccharomyces cerevisiae* of weak-acid preservatives, uncouplers, and medium-chain fatty acids. *FEMS Microbiology letters* **142**: 53–8.

**Sun L, Zeng X, Yan C, Sun X, Gong X, Rao Y, Yan N. 2012.** Crystal structure of a bacterial homologue of glucose transporters GLUT1-4. *Nature* **490**: 361–6.

**Teixeira MC, Cabrito TR, Brazão J, Sá-Correia I. 2013.** Yeast as model eukaryote and expression host system. *Sociedade Portuguesa de Microbiologia*.

**Teixeira MC, Duque P, Sá-Correia I. 2007.** Environmental genomics: mechanistic insights into toxicity of and resistance to the herbicide 2,4-D. *Trends in biotechnology* **25**: 363–70.

**Teixeira MC, Sá-Correia I. 2002.** *Saccharomyces cerevisiae* Resistance to Chlorinated Phenoxyacetic Acid Herbicides Involves Pdr1p-Mediated Transcriptional Activation of TPO1 and PDR5 Genes. **537**: 530–537.

**Tenreiro S, Nunes P a, Viegas C a, Neves MS, Teixeira MC, Cabral MG, Sá-Correia I. 2002.** AQR1 Gene (ORF YNL065w) encodes a plasma membrane transporter of the major facilitator superfamily that confers resistance to short-chain monocarboxylic acids and quinidine in *Saccharomyces cerevisiae*. *Biochemical and Biophysical Research Communications* **292**: 741–8.

**Tenreiro S, Rosa PC, Viegas C a, Sá-Correia I. 2000.** Expression of the AZR1 Gene (ORF YGR224w), encoding a plasma membrane transporter of the major facilitator superfamily, is required for adaptation to acetic acid and resistance to azoles in *Saccharomyces cerevisiae*. *Yeast (Chichester, England)* **16**: 1469–81.

**Tenreiro S, Vargas RC, Teixeira MC, Magnani C, Sá-Correia I. 2005.** The yeast multidrug transporter Qdr3 (Ybr043c): localization and role as a determinant of resistance to quinidine, barban, cisplatin, and bleomycin. *Biochemical and Biophysical Research Communications* **327**: 952–9.

- Tirosh O, Sigal N, Gelman A, Sahar N, Fluman N, Siemion S, Bibi E. 2012.** Manipulating the drug/proton antiport stoichiometry of the secondary multidrug transporter MdfA. *Proceedings of the National Academy of Sciences of the United States of America* **109**: 12473–8.
- Tomitori H, Kashiwagi K, Asakawa T, Kakinuma Y, Michael AJ, Igarashi K. 2001.** Multiple polyamine transport systems on the vacuolar membrane in yeast. *The Biochemical journal* **353**: 681–8.
- Ton V-K, Rao R. 2004.** Functional expression of heterologous proteins in yeast: insights into Ca<sup>2+</sup> signaling and Ca<sup>2+</sup>-transporting ATPases. *American journal of Physiology. Cell Physiology* **287**: C580–9.
- Truernit E, Schmid J, Epple P, Illig J, Sauer N. 1996.** The sink-specific and stress-regulated Arabidopsis STP4 Gene: enhanced expression of a Gene encoding a monosaccharide transporter by wounding, elicitors, and pathogen challenge. *The Plant Cell* **8**: 2169–82.
- Truernit E, Stadler R, Baier K, Sauer N. 1999.** A male gametophyte-specific monosaccharide transporter in Arabidopsis. *The Plant Journal* **17**: 191–201.
- Tsay Y-F, Chiu C-C, Tsai C-B, Ho C-H, Hsu P-K. 2007.** Nitrate transporters and peptide transporters. *FEBS letters* **581**: 2290–300.
- Do Valle Matta MA, Jonniaux JL, Balzi E, Goffeau A, van den Hazel B. 2001.** Novel target Genes of the yeast regulator Pdr1p: a contribution of the TPO1 Gene in resistance to quinidine and other drugs. *Gene* **272**: 111–9.
- Vargas RC, Tenreiro S, Teixeira MC, Fernandes AR, Sa I. 2004.** Saccharomyces cerevisiae Multidrug Transporter Qdr2p (Yil121wp): Localization and Function as a Quinidine Resistance Determinant. *Antimicrobial Agents and Chemotherapy* **48**: 2531–2537.
- Vargas RC, García-Salcedo R, Tenreiro S, Teixeira MC, Fernandes AR, Ramos J, Sá-Correia I. 2007.** Saccharomyces cerevisiae multidrug resistance transporter Qdr2 is implicated in potassium uptake, providing a physiological advantage to quinidine-stressed cells. *Eukaryotic cell* **6**: 134–42.
- Velasco I, Tenreiro S, Calderon IL, Andre B, Gene D De. 2004.** Saccharomyces cerevisiae Aqr1 Is an Internal-Membrane Transporter Involved in Excretion of Amino Acids. **3**: 1492–1503.
- Versaw WK, Harrison MJ, Samuel T, Noble R, Parkway SN. 2002.** A Chloroplast Phosphate Transporter, PHT2; 1, Influences Allocation of Phosphate within the Plant and Phosphate-Starvation Responses. *Plant Cell* **14**: 1751–1766.

- Vicente-Agullo F, Rigas S, Desbrosses G, Dolan L, Hatzopoulos P, Grabov A. 2004.** Potassium carrier TRH1 is required for auxin transport in Arabidopsis roots. *The Plant Journal: for Cell and Molecular Biology* **40**: 523–35.
- Unkles SE, Hawker KL, Grieve C, Campbell EI, Montague P, Kinghorn JR. 1991.** crnA encodes a nitrate transporter in Aspergillus nidulans. *Proceedings of the National Academy of Sciences of the United States of America* **88**: 204–8.
- White P, Broadley M. 2000.** Mechanisms of caesium uptake by plants. *New phytologist*: 241–256.
- Wilson-O'Brien AL, Patron N, Rogers S. 2010.** Evolutionary ancestry and novel functions of the mammalian glucose transporter (GLUT) family. *BMC evolutionary biology* **10**: 152.
- Woodward AW, Bartel B. 2005.** Auxin: regulation, action, and interaction. *Annals of Botany* **95**: 707–35.
- Yan N. 2013.** Structural advances for the major facilitator superfamily (MFS) transporters. *Trends in Biochemical Sciences* **38**: 151–9.
- Yang H, Murphy AS. 2009.** Functional expression and characterization of Arabidopsis ABCB, AUX 1 and PIN auxin transporters in Schizosaccharomyces pombe. *The Plant Journal: for Cell and Molecular Biology* **59**: 179–91.
- Yang Y, Hammes UZ, Taylor CG, Schachtman DP, Nielsen E. 2006.** High-Affinity Auxin Transport by the AUX1 Influx Carrier Protein. *Current Biology* **16**: 1123–1127.
- Yesilirmak F, Sayers Z. 2009.** Heterologous expression of plant Genes. *International Journal of Plant Genomics* **2009**: 296482.